Search for prompt production of pentaquarks in charm hadron final states

R. Aaij *et al.*[*]
(LHCb Collaboration)

(Received 11 April 2024; accepted 3 June 2024; published 1 August 2024)

A search for hidden-charm pentaquark states decaying to a range of $\Sigma_c\bar{D}$ and $\Lambda_c^+\bar{D}$ final states, as well as doubly charmed pentaquark states to $\Sigma_c D$ and $\Lambda_c^+ D$, is made using samples of proton-proton collision data corresponding to an integrated luminosity of 5.7 fb^{-1} recorded by the LHCb detector at $\sqrt{s} = 13$ TeV. Since no significant signals are found, upper limits are set on the pentaquark yields relative to that of the Λ_c^+ baryon in the $\Lambda_c^+ \to pK^-\pi^+$ decay mode. The known pentaquark states are also investigated, and their signal yields are found to be consistent with zero in all cases.

DOI: 10.1103/PhysRevD.110.032001

I. INTRODUCTION

Since the formulation of the quark model [1,2], hadronic states beyond the conventional $q\bar{q}$ mesons and qqq baryons have been proposed. Hadrons with different combinations of quarks q and gluons g, such as pentaquarks ($q\bar{q}qqq$), tetraquarks ($q\bar{q}q\bar{q}$) [1,2], six-quark H-dibaryons ($q\bar{q}q\bar{q}q\bar{q}$) [3], hybrids ($q\bar{q}g$) [4] and glueballs (ggg) [5], have been predicted by QCD-based models. The existence of such "exotic" hadrons had been debated for several years without a consensus being reached. In the early 2000s, new hadrons with unexpected features were observed, such as the $D_{s0}^*(2317)^+$ [6] and $\chi_{c1}(3872)$ [7] mesons, followed shortly after by the discovery of many other charmonium-like and bottomoniumlike states. While it is still not possible to rule out firmly a conventional nature for the majority of such states, the observation of manifestly exotic hadrons such as the $Z_c(4430)^+$ meson [8], an electrically charged charmoniumlike state, three P_c^+ baryons [9–11], with a minimal quark content $c\bar{c}uud$, and the T_{cc}^+ state [12,13], a meson containing two charm quarks, established the existence of QCD exotics. Many models have been proposed to explain the exotic nature of such states: *hadronic molecules* [14,15], whose constituents are color-singlet hadrons bound by residual nuclear forces; *tetraquarks and pentaquarks* [16,17], bound states where diquarks and diantiquarks are building blocks; *hadro-quarkonium* [18], a cloud of light quarks and gluons bound to a heavy $Q\bar{Q}$ core state via van der Waals forces (Q represents a heavy quark, such as the b quark), and *threshold effects*, enhancements caused by threshold cusps or rescattering processes [19,20]. An intriguing feature of many exotic hadrons is the proximity to hadron-hadron thresholds. For example, the three pentaquark states $P_c(4312)^+$, $P_c(4440)^+$ and $P_c(4457)^+$, observed in the $J/\psi p$ projection of $\Lambda_b^0 \to J/\psi p K^-$ decays [11], have masses that are just below the $\Sigma_c^+\bar{D}^0$ and $\Sigma_c^+\bar{D}^{*0}$ thresholds.[1] More experimental and theoretical scrutiny is required to understand if this is just coincidental or related to the internal structure of the states as bound systems of a baryon and a meson. As for the conventional hadrons, the observation of new decay modes can shed light on the binding mechanism of exotic hadrons. In addition, many models predict doubly charmed pentaquark states, where doubly charmed refers to a state with two units of charm quantum number, decaying to a range of $\Sigma_c\ D$ and $\Lambda_c^+\ D$ combinations [21]. Excited Ξ_{cc} baryons could be observed in such final states as well [22].

This paper presents a search for the $P_c(4312)^+$, $P_c(4440)^+$ and $P_c(4457)^+$ baryons and other pentaquarks with hidden charm, meaning charm quantum number equal to zero, in the prompt $\Sigma_c\bar{D}^{(*)}$, $\Sigma_c^*\bar{D}^{(*)}$, $\Lambda_c^+\bar{D}^{(*)}$, and $\Lambda_c^+\pi\bar{D}^{(*)}$ mass spectra.[2] A search for pentaquarks containing two charm quarks has also been carried out in the $\Sigma_c D^{(*)}$, $\Sigma_c^* D^{(*)}$, $\Lambda_c^+ D^{(*)}$ and $\Lambda_c^+\pi D^{(*)}$ mass spectra. Upper limits on the yields in these spectra relative to the $\Lambda_c^+ \to pK^-\pi^+$ normalization channel are presented. The measurements are based on samples of proton-proton (pp) collision data corresponding to an integrated luminosity of 5.7 fb^{-1} at center-of-mass energies of 13 TeV recorded by the LHCb experiment between 2016 and 2018.

[*]Full author list given at the end of the article.

[1]The $\Sigma_c(2455)$ and $\Sigma_c(2520)$ baryons are referred to as Σ_c and Σ_c^*, respectively.

[2]The inclusion of charge-conjugate processes is implied throughout.

II. THE LHCb DETECTOR

The LHCb detector [23,24] is a single-arm forward spectrometer covering the pseudorapidity range $2 < \eta < 5$, designed for the study of particles containing b or c quarks. The detector includes a high-precision tracking system consisting of a silicon-strip vertex detector surrounding the pp interaction region, a large-area silicon-strip detector located upstream of a dipole magnet with a bending power of about 4 Tm and three stations of silicon-strip detectors and straw drift tubes placed downstream of the magnet. The tracking system provides a measurement of the momentum p of charged particles with a relative uncertainty that varies from 0.5% at low momentum to 1.0% at 200 GeV/c. The minimum distance of a track to a primary pp collision vertex (PV), the impact parameter, is measured with a resolution of $(15 + 29/p_{\mathrm{T}})$ μm, where p_{T} is the component of the momentum transverse to the beam, in GeV/c. Different types of charged hadrons are distinguished using information from two ring-imaging Cherenkov detectors. Photons, electrons and hadrons are identified by a calorimeter system consisting of scintillating-pad and preshower detectors, an electromagnetic and a hadronic calorimeter. Muons are identified by a system composed of alternating layers of iron and multiwire proportional chambers.

The online event selection is performed by a trigger, which consists of a hardware stage followed by a two-level software stage [25]. At the hardware trigger stage, events are required to have a muon with high p_{T} or hadron, photon or electron with high transverse energy in the calorimeters. In between the two software trigger stages, an alignment and calibration of the detector is performed in near real time and their results are used in the trigger [26]. The same alignment and calibration information is propagated to the offline reconstruction, ensuring consistent and high-quality particle identification (PID) information between the trigger and offline software. The identical performance of the online and offline reconstruction offers the opportunity to perform physics analyses directly using candidates reconstructed in the trigger [27,28]. This analysis exploits this by using D^0, D^+ and Λ_c^+ candidates fully reconstructed in the trigger, as well as single pions for certain final states.

Simulated pp collisions are generated using PYTHIA [29] with a specific LHCb configuration [30]. Decays of hadronic particles are described by EVTGEN [31], in which final-state radiation is generated using PHOTOS [32]. The interaction of the generated particles with the detector, and its response, are implemented using the GEANT4 toolkit [33] as described in Ref. [34].

III. SELECTION

All signal mode combinations are listed in Table I. It is interesting to note that the quark content of each of these states is comparable to the quark content of the $J/\psi p$ combination ($c\bar{c}uud$), since all combinations consist of only the up, down and charm quarks. In the selection process, open-charm hadrons are selected by the trigger. The Λ_c^+ baryon is reconstructed in the $\Lambda_c^+ \to pK^-\pi^+$ decay mode for both signal and normalization channels, the D^0 meson in the decay $D^0 \to K^-\pi^+$ and the D^+ meson in the decay $D^+ \to K^-\pi^+\pi^+$. To improve the signal purity, stringent PID and vertex quality requirements are imposed. To further suppress the background in the Λ_c^+ decay mode, the gradient-boosted decision tree classifier trained on data for the analysis described in Ref. [35] is used. This identifies Λ_c^+ candidates with high efficiency by combining information on the vertex quality and the PID. The classifier is applied directly in the case of the modes

TABLE I. All possible combinations of Σ_c or Λ_c^+ baryons with $D^{(*)}$ mesons to produce the isospin multiplet. Combinations of Λ_c^+ baryons, pions and D mesons are also considered. From each Σ_c D combination the corresponding $\Lambda_c^+\pi D$ combination can be derived. The charge of the corresponding pentaquark state is given, along with the isospin, hypercharge and charm quantum numbers. The last column indicates whether a mode has an upper limit set in this paper. The combinations are split by the charm value.

Hadron 1	Hadron 2	Charge	I_3	Y	C	Limit set
Λ_c^+	$\bar{D}^0$	+1	1/2	1	0	✓
Λ_c^+	D^-	0	−1/2	1	0	✓
Λ_c^+	D^{*-}	0	−1/2	1	0	✓
Σ_c^{++}	$\bar{D}^0$	+2	3/2	1	0	✓
Σ_c^{++}	D^-	+1	1/2	1	0	✓
Σ_c^{++}	D^{*-}	+1	1/2	1	0	×
Σ_c^0	$\bar{D}^0$	0	−1/2	1	0	✓
Σ_c^0	D^-	−1	−3/2	1	0	✓
Σ_c^0	D^{*-}	−1	−3/2	1	0	×
Σ_c^{*++}	$\bar{D}^0$	+2	3/2	1	0	✓
Σ_c^{*++}	D^-	+1	1/2	1	0	✓
Σ_c^{*++}	D^{*-}	+1	1/2	1	0	✓
Σ_c^{*0}	$\bar{D}^0$	0	−1/2	1	0	✓
Σ_c^{*0}	D^-	−1	−3/2	1	0	✓
Σ_c^{*0}	D^{*-}	−1	−3/2	1	0	✓
Λ_c^+	D^0	+1	−1/2	3	2	✓
Λ_c^+	D^+	+2	1/2	3	2	✓
Λ_c^+	D^{*+}	+2	1/2	3	2	✓
Σ_c^{++}	D^0	+2	1/2	3	2	×
Σ_c^{++}	D^+	+3	3/2	3	2	×
Σ_c^{++}	D^{*+}	+3	3/2	3	2	×
Σ_c^0	D^0	0	−3/2	3	2	×
Σ_c^0	D^+	+1	−1/2	3	2	×
Σ_c^0	D^{*+}	+1	−1/2	3	2	×
Σ_c^{*++}	D^0	+2	1/2	3	2	✓
Σ_c^{*++}	D^+	+3	3/2	3	2	✓
Σ_c^{*++}	D^{*+}	+3	3/2	3	2	×
Σ_c^{*0}	D^0	0	−3/2	3	2	✓
Σ_c^{*0}	D^+	+1	−1/2	3	2	✓
Σ_c^{*0}	D^{*+}	+1	−1/2	3	2	×

involving a direct Λ_c^+ decay and is used as an input to the multivariate algorithm that is used to select Σ_c candidates in the $\Sigma_c \to \Lambda_c^+\pi^\pm$ decay mode. In Fig. 1 the invariant mass distribution for each of these open-charm hadrons is shown. Candidate D^* (Σ_c) hadrons are built by combining the D^0 (Λ_c^+) candidates with a well-identified charged pion with p_T above 200 MeV/c.

To improve the purity of the Σ_c selection, a multilayer perceptron algorithm provided by the TMVA package [36] is trained using the $\Sigma_c^{++} \to \Lambda_c^+\pi^+$ simulated signal sample and a data sample at high mass, well above the expected signal, in order to describe the shape of the combinatoric background events. As input, the network uses the p_T and rapidity of the pion and of the Σ_c^{++} and Λ_c^+ baryons, together with information on the pion PID and the Λ_c^+ classifier response described above.

Once the corresponding baryon and meson combinations have been built, the signal regions are selected. These regions are based on fits to the baryon and meson spectra and require the mass is within a 3σ window around the mean mass value found from the fits, where σ is the resolution of the signal peak. These regions are dependent on the baryon and meson combination the signal mode consists of. The chosen windows are highlighted in Fig. 1. The background regions are selected as a wider window around the fitted mean value to accurately describe the background as close to the signal

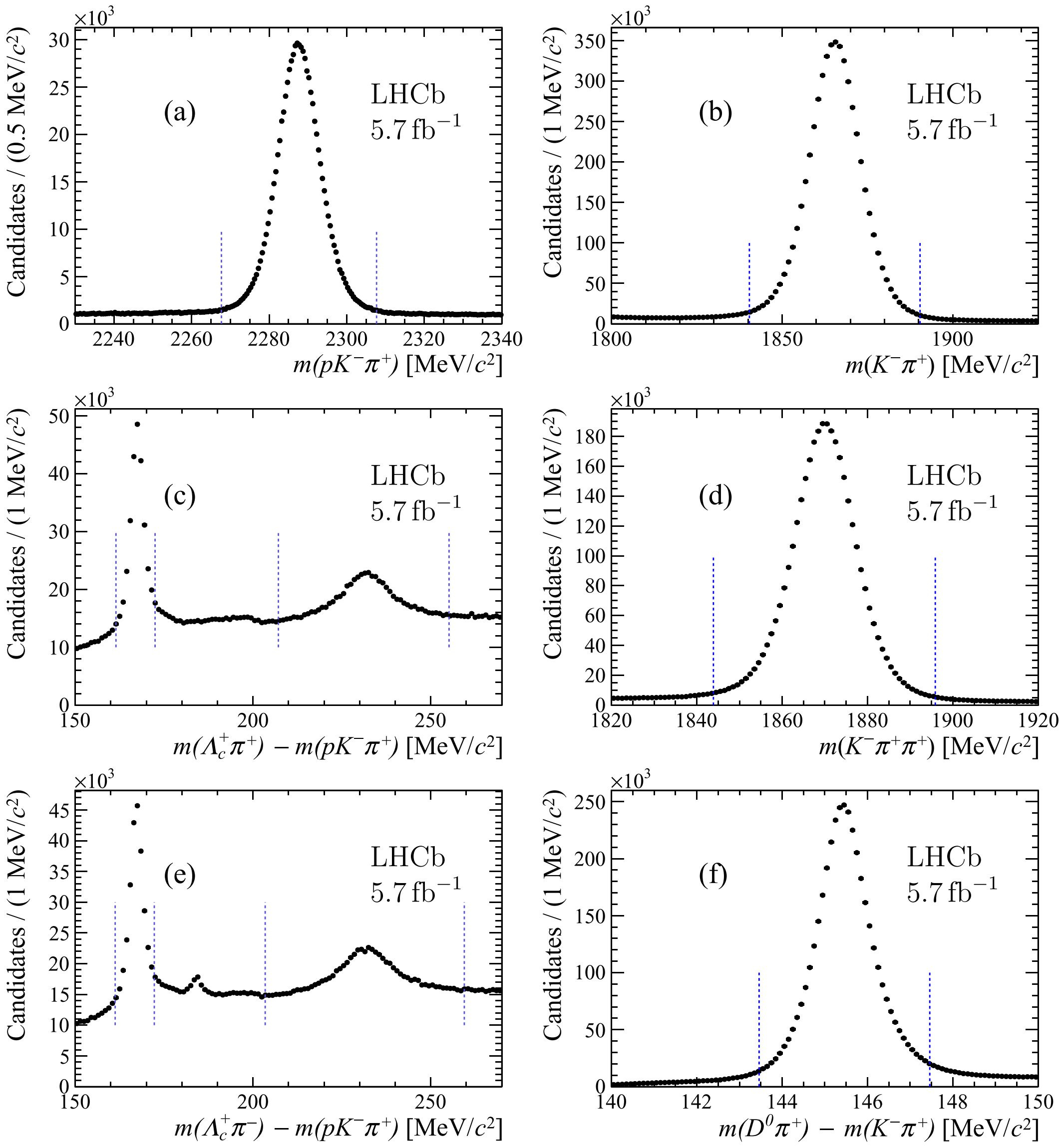

FIG. 1. Invariant mass distributions of the (a) $\Lambda_c^+ \to pK^-\pi^+$, (b) $D^0 \to K^-\pi^+$, (c) $\Sigma_c^{(*)++} \to \Lambda_c^+\pi^+$, (d) $D^+ \to K^-\pi^+\pi^+$, (e) $\Sigma_c^{(*)0} \to \Lambda_c^+\pi^-$ and (f) $D^{*+} \to D^0\pi^+$ decays. Note that in (c), (e) and (f) the mass of the charm hadron is subtracted from the mass distribution to minimize detector resolution effects. In (e) a contribution can also be seen at around 185 MeV/c^2 from the fully reconstructed $\Xi_c^0 \to \Lambda_c^+\pi^-$ decay. The blue dashed lines show the chosen signal windows around the peaks.

region as possible. This corresponds to a 3–4.5σ window around the fitted mean value of the mass. Selection criteria are applied on the opening angle between each pair of charged particles to ensure there are no candidates where the same track is used multiple times. If two or more candidates are selected, all but one candidate is discarded at random. Any signal combinations with fewer than 30 candidates within the mass range of interest are not analyzed further. This corresponds to ten modes in total, as summarized in Table I. Note that all $\Lambda_c^+ D \pi$ combinations exceed this threshold.

IV. LIMIT SETTING PROCEDURE

For each mode, a kinematic fit is done to constrain the mass of intermediate charm hadrons to their known values and to constrain them to originate at the same PV. The Q-value spectrum, where the mass of each charmed hadron from the kinematic fit is subtracted from the decaying particle, is fitted using a simultaneous extended unbinned maximum-likelihood fit to the background and signal regions, where the background shape is shared between the two. The background normalization region is a combination of the upper and lower sideband regions and for the $\Sigma_c D$ and $\Sigma_c^* D$ modes is selected from the Σ_c sideband region. For the $\Lambda_c^+ \pi D$ and $\Lambda_c^+ D$ modes the background region used is from the Λ_c^+ sideband region. For the $\Sigma_c D$, $\Sigma_c^* D$ and $\Lambda_c^+ \pi D$ modes, the background model used is a threshold function with all parameters shared between signal and sideband regions, while for the $\Lambda_c^+ D$ D modes, the background model is the sum of a first-order Chebyshev polynomial and a log-normal distribution with all parameters shared between signal and sideband regions apart from the fraction between the two functions, which is independent. An example of the fit in the background-only hypothesis for each signal mode category ($\Sigma_c D$, $\Sigma_c^* D$, $\Lambda_c^+ D$ and $\Lambda_c^+ \pi D$) and the corresponding background is shown in Fig. 2. Four different signal models are investigated: one using a Gaussian function, where the resolution is fixed to the detector resolution found using simulation, and three using Voigtian functions, built from the convolution of the same Gaussian function with a Breit-Wigner distribution, with fixed widths of 5, 10 and 15 MeV/c^2, in order to provide greater sensitivity to pentaquark states with broader width. Larger widths are not considered, since the pentaquark states are predicted to be narrow [15].

The invariant mass distribution of $\Lambda_c^+ \to p K^- \pi^+$ candidates (the normalization channel) is shown in Fig. 3. The distribution is fitted using the sum of a Gaussian function with a Crystal Ball function [37] for the signal model and a first-order Chebyshev polynomial for the background. The obtained signal yield is $789\,200 \pm 1300$.

To search for possible pentaquark contributions, a scan of the Q-value distribution in each signal mode is made from the kinematic threshold up to 600 MeV/c^2 in steps of 4 MeV/c^2, which corresponds roughly to the signal resolution. At each point, an extended unbinned maximum-likelihood fit is performed. The local p value is determined from the difference between the negative log-likelihood of each fit and a fit with the background-only hypothesis and is assumed to be a one-tailed distribution. An example of the p-value distribution across the scan range is shown for each signal category for the $\Lambda_c^+ \pi^- \bar{D}^0$ mode in Fig. 4. The minimum local p value in each channel varies from 0.041 in the $\Sigma_c^{*++} D^{*-}$ channel with the Voigtian signal model with a 15 MeV/c^2 width, to 3.36×10^{-6} in the $\Lambda_c^+ \pi^+ D^-$ channel with the Voigtian signal model with a 15 MeV/c^2 width. The latter corresponds to a local significance of 4.50σ.

The local p value is corrected in order to account for the look-elsewhere effect [38] (LEE) using

$$p_{\mathrm{corr}} = p_{\mathrm{loc}} + \langle N(c_0) \rangle \exp\left(-\frac{c - c_0}{2}\right), \tag{1}$$

where p_{corr} and p_{loc} are the corrected and local p value, respectively, c is the profile likelihood ratio $2\Delta \ln \mathcal{L}$, and c_0 is a reference level set to 0.5 where the average number of "upcrossings" $\langle N(c_0) \rangle$ is found. An upcrossing is defined as when the profile likelihood ratio crosses the chosen threshold with a positive slope. The corrected p value varies from 1 (corresponding to no observation of any significant signal) in many channels, to 1.45×10^{-4} in the $\Lambda_c^+ \pi^+ D^-$ channel with the Voigtian signal model where the width is set to 15 MeV/c^2. To evaluate the interpretation of these p values the scanning procedure is repeated using 1000 background-only pseudoexperiments for each channel and the Voigtian signal model with a width of 15 MeV/c^2. The average number of fluctuations above 3σ significance across all channels is 7.0 with a standard deviation of 5.0. In the data, five channels, namely the $\Lambda_c^+ \pi^+ \bar{D}^0$, $\Lambda_c^+ \pi^+ D^-$, $\Lambda_c^+ \pi^- \bar{D}^0$, $\Lambda_c^+ \pi^- D^-$ and $\Lambda_c^+ \pi^- D^+$ channels, are observed with local significances greater than 3σ, obtained with the Voigtian signal model with a width of 15 MeV/c^2. Thus, we conclude that these significances are consistent with background fluctuations, as determined in the study with pseudoexperiments.

The previously observed pentaquark states are also investigated, namely the $P_c(4312)^+$, $P_c(4440)^+$ and $P_c(4457)^+$ states. This is only carried out for states with the same total charge and hidden-charm quark content. By setting the mass and width in the Voigtian function to the known values of these states [11] and carrying out the same fitting procedure previously described, the significance of the states is found, and the limits are set using the procedure described below.

In this study, several sources of systematic uncertainties are considered. Since the number of tracks is different for signal and normalization, an important source of systematic uncertainty is due to the knowledge of the tracking efficiency, which is affected by hadronic interactions in the detector and overlaps between tracks or occupancy.

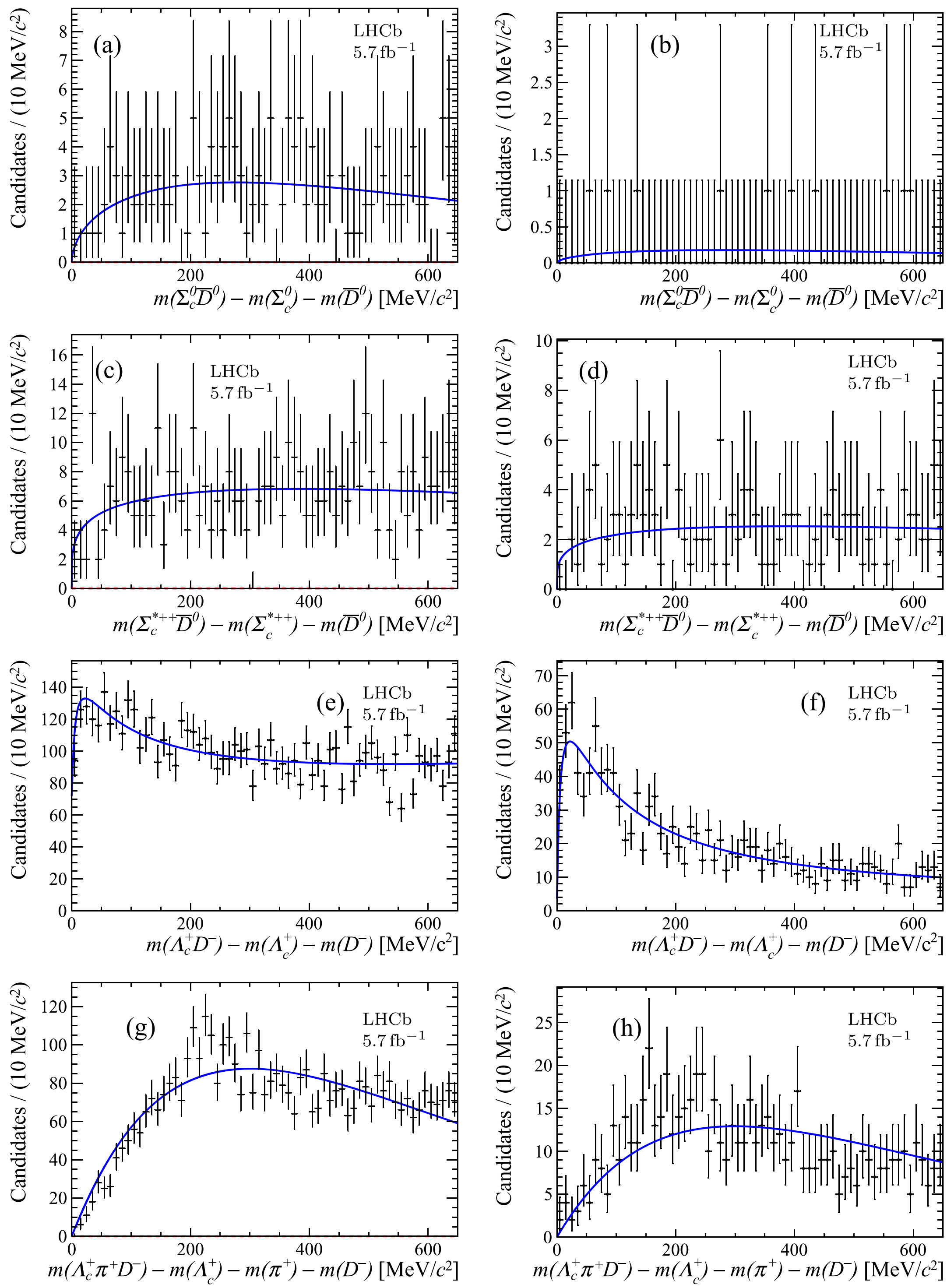

FIG. 2. Distributions of the Q-value spectra for the $\Sigma_c^0\ \bar{D}^0$ (a) signal and (b) background regions, for the $\Sigma_c^{*++}\ \bar{D}^0$ (c) signal and (d) background regions, the $\Lambda_c^+\ D^-$ (e) signal and (f) background regions and the $\Lambda_c^+\ \pi^+\ D^-$ (g) signal and (h) background regions. The fits for the background-only hypotheses are overlaid.

Further uncertainties arise and are quantified from possible differences in the reconstruction between data and simulation, such as differences in selection and PID efficiencies. The performance of the classifier for the Σ_c baryon and the behavior of the trigger in data and simulation are also considered as sources of uncertainty. The knowledge of the branching fractions of the decay modes used leads to a further uncertainty [39]. The effect of varying the

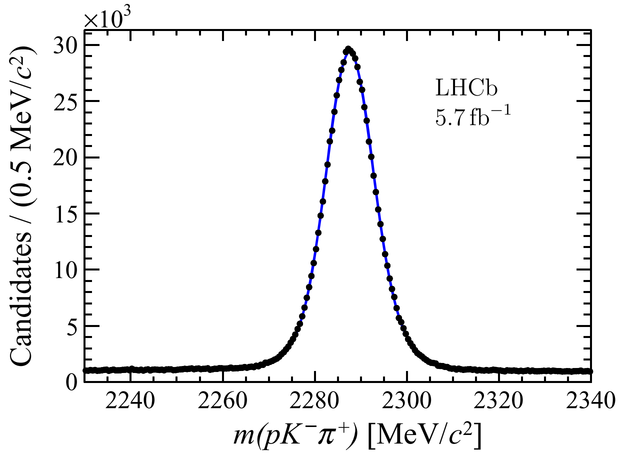

FIG. 3. Invariant mass distribution of the $\Lambda_c^+ \to pK^-\pi^+$ decay. The fit results are overlaid.

background model on the signal yield is also investigated, e.g., by using either a threshold function or Chebyshev polynomial summed with a log-normal distribution or by varying which background parameters are shared between the signal and background regions. This is done for the combination with the highest signal yield, and the uncertainty is applied for all signal combinations. The range of values found for each contribution is summarized in Table II.

An upper limit (UL) is set on $R(\Lambda_c^+)$, which is defined as

$$R(\Lambda_c^+) = \frac{N_P}{N_{\Lambda_c^+}} \times \frac{\epsilon_{\Lambda_c^+}}{\epsilon_P}, \tag{2}$$

where N represents the Λ_c^+ or pentaquark (P) yield and ϵ is the combined trigger and selection efficiency as found

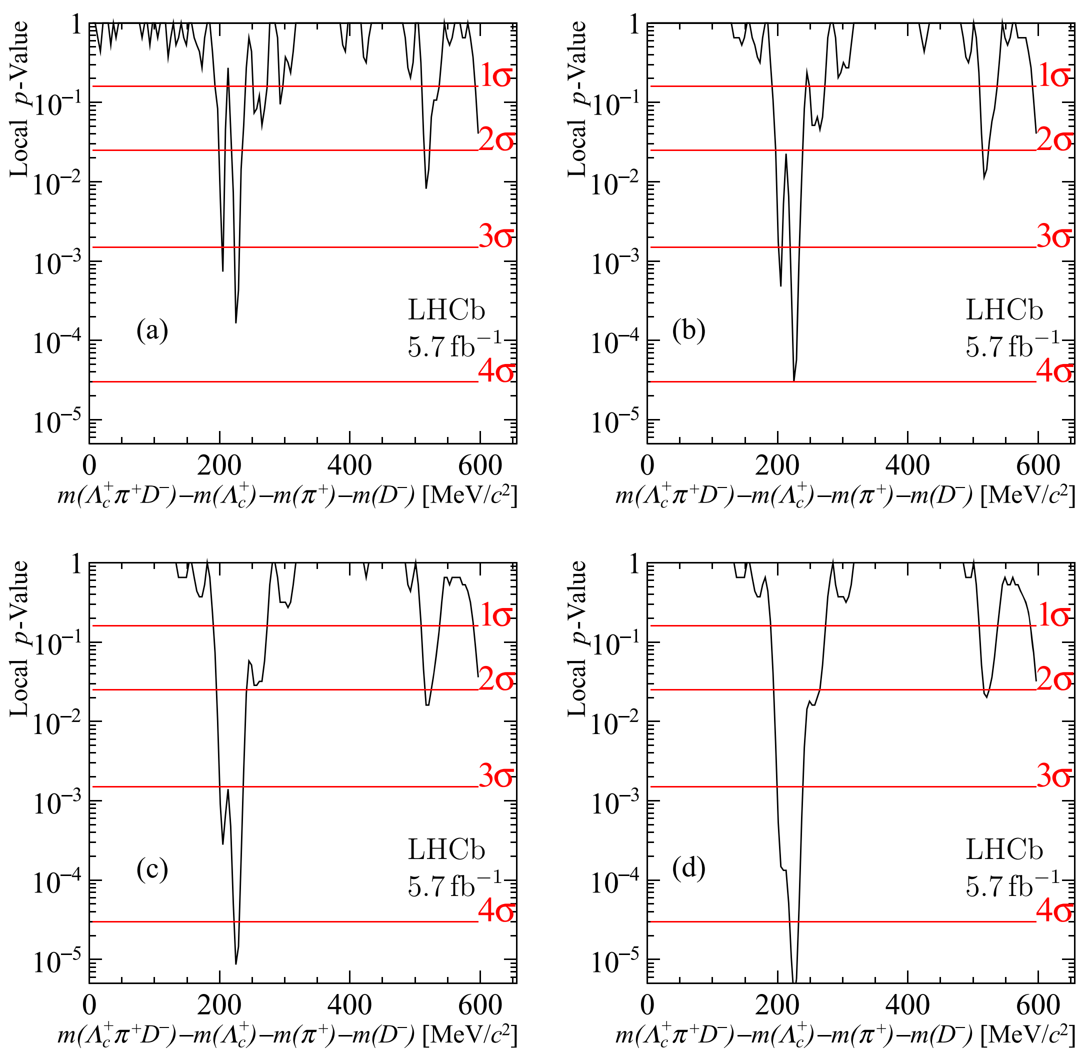

FIG. 4. Local p-value distributions for the $\Lambda_c^+\ \pi^+\ D^-$ mode with different signal models: (a) Gaussian function, (b) Voigtian function with 5 MeV/c^2 width, (c) Voigtian function with 10 MeV/c^2 width, and (d) Voigtian function with 15 MeV/c^2 width. The red lines correspond to the levels of local significance.

TABLE II. Range of values of each systematic uncertainty contribution and the total combination for the different signal modes.

Source	Uncertainty (%)
Tracking	3.00–6.20
Reconstruction efficiency	0.70–3.70
Generation efficiency	0.10–0.20
Σ_c classifier performance	0.54
L0 trigger efficiency	1.40–7.90
Branching fraction	0.01–0.03
Background model	11.6
Total	12.10–15.79

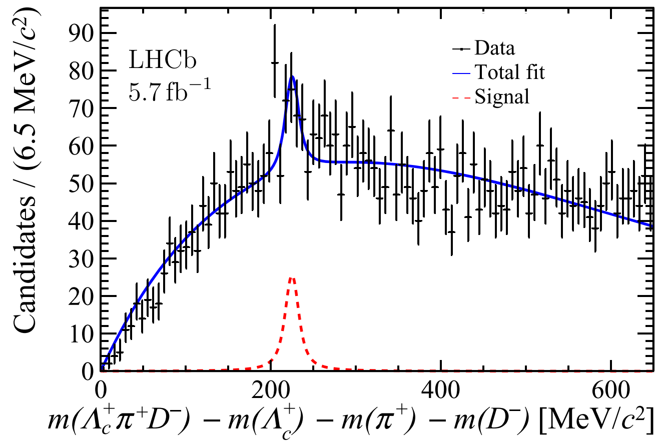

FIG. 6. Distribution of the Q value in the $\Lambda_c^+ \pi^+ D^-$ channel, where the most significant signal is seen. The fit result is overlaid.

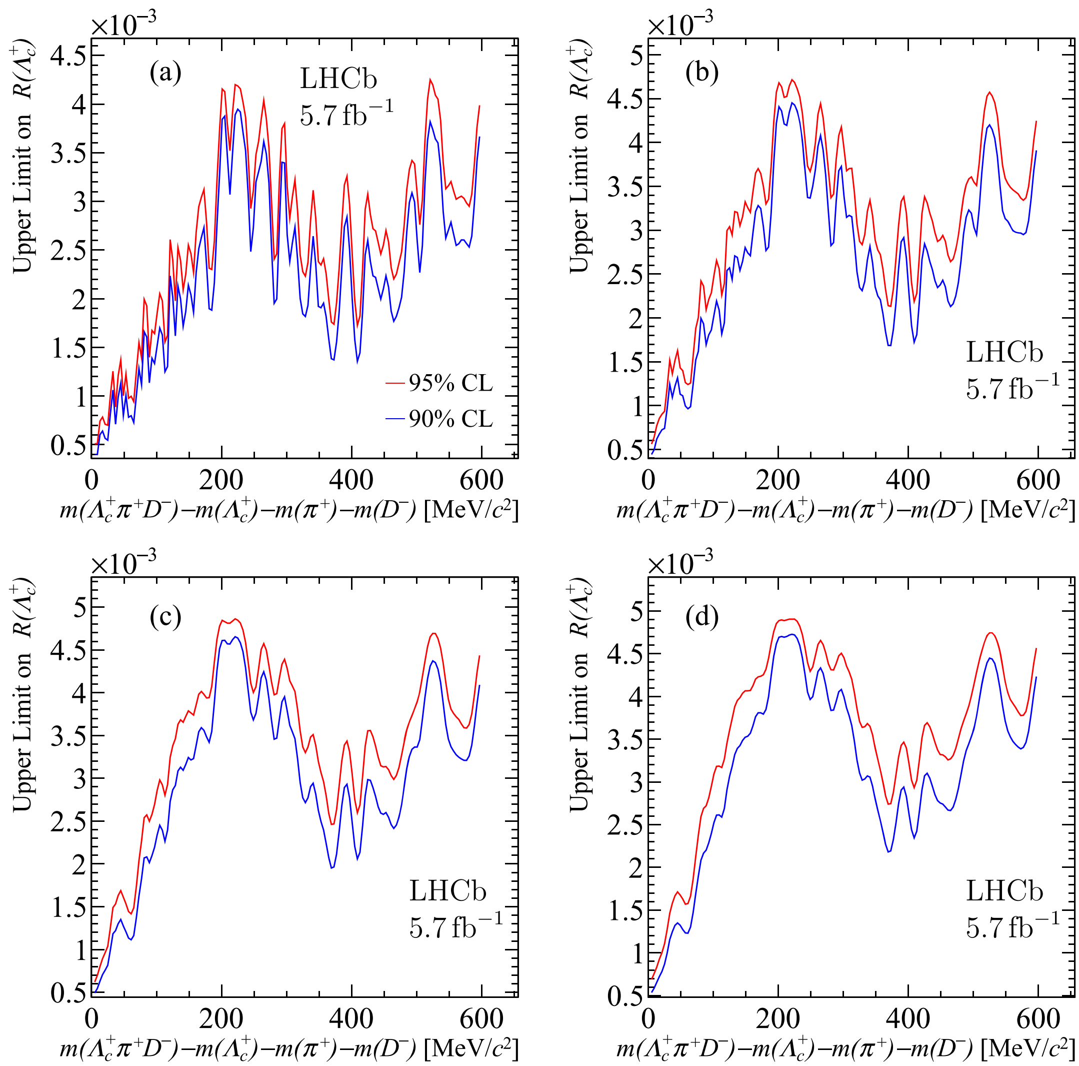

FIG. 5. Upper limits on $R(\Lambda_c^+)$ distribution, at 90% and 95% CL, for the $\Lambda_c^+ \pi^+ D^-$ mode with different signal models: (a) Gaussian function, (b) Voigtian function with 5 MeV/c^2 width, (c) Voigtian function with 10 MeV/c^2 width, and (d) Voigtian function with 15 MeV/c^2 width.

TABLE III. Upper limits on $R(\Lambda_c^+)$ at 90% and 95% CL for the modes with the same total charge as the known pentaquark states and with hidden-charm quark content. The local p value and significance are listed as well as the signal yield, where the error on the signal yield is statistical only.

Decay mode	Pentaquark hypothesis	p value	Significance (σ)	Signal yield	Upper limit ($\times 10^{-3}$) (90% CL)	(95% CL)
$\Lambda_c^+ \bar{D}^0$	$P_c(4312)^+$	0.32	0.48	19.78 ± 22.27	1.17	1.29
	$P_c(4440)^+$	0.44	0.15	26.91 ± 28.17	1.41	1.53
	$P_c(4457)^+$	0.53	0.00	6.20 ± 13.60	1.27	1.43
$\Lambda_c^+ \pi^+ D^{*-}$	$P_c(4440)^+$	1.00	0.00	0.00 ± 0.96	0.72	0.91
	$P_c(4457)^+$	1.00	0.00	0.00 ± 1.73	0.77	0.97
$\Lambda_c^+ \pi^- D^{*-}$	$P_c(4440)^+$	1.00	0.00	0.00 ± 0.80	0.63	0.80
	$P_c(4457)^+$	1.00	0.00	0.00 ± 0.74	0.59	0.74
$\Lambda_c^+ \pi^+ D^-$	$P_c(4312)^+$	1.00	0.00	0.00 ± 1.56	0.69	0.88
	$P_c(4440)^+$	0.65	0.00	4.43 ± 11.67	3.71	4.24
	$P_c(4457)^+$	0.65	0.00	5.94 ± 12.68	3.13	3.61
$\Lambda_c^+ \pi^- D^-$	$P_c(4312)^+$	1.00	0.00	0.00 ± 1.42	0.67	0.86
	$P_c(4440)^+$	0.53	0.00	12.52 ± 15.89	3.91	4.37
	$P_c(4457)^+$	0.53	0.00	8.60 ± 12.22	3.10	3.51
$\Sigma_c^0 D^-$	$P_c(4440)^+$	1.00	0.00	0.00 ± 2.47	0.82	1.03
	$P_c(4457)^+$	1.00	0.00	0.00 ± 1.05	0.63	0.81
$\Sigma_c^{++} D^-$	$P_c(4440)^+$	0.80	0.00	0.61 ± 4.52	1.13	1.37
	$P_c(4457)^+$	0.59	0.00	0.66 ± 1.79	0.80	0.99
$\Sigma_c^{*0} D^-$	$P_c(4440)^+$	0.31	0.49	3.23 ± 3.53	1.89	2.24
	$P_c(4457)^+$	1.00	0.00	0.00 ± 3.09	0.91	1.13
$\Sigma_c^{*++} D^-$	$P_c(4440)^+$	0.75	0.00	1.20 ± 3.81	1.38	1.67
	$P_c(4457)^+$	1.00	0.00	0.00 ± 5.74	0.87	1.08

using simulated events. The limit is then determined at 90% and 95% confidence levels (CL). The likelihood profile is assumed to be parabolic and is determined for five equal-sized steps in the signal yield around the value found from the fit. It is then convolved with a Gaussian function with a mean of zero and a width set to $\sigma = \sigma_{\rm syst} \cdot \mu$, where $\sigma_{\rm syst}$ is the systematic uncertainty on the signal yield and μ is the most probable signal yield. The convolved function takes the form

$$L(N') = \int_0^\infty L(N) \frac{1}{\sqrt{2\pi}\sigma} \exp\left(\frac{-(N-N')^2}{2\sigma^2}\right) dN, \quad (3)$$

where $L(N)$ is the normalized likelihood function. This likelihood profile is numerically integrated to find the value of the integral at 90% or 95% of the physical region, corresponding to the 90% and 95% CL upper limits on the signal yield, and is then converted to an upper limit on $R(\Lambda_c^+)$ using Eq. (2). An example of the upper limit for each signal category is shown for the $\Lambda_c^+ \pi^- \bar{D}^0$ mode in Fig. 5.

The results for the scan across the Q-value spectrum in each signal combination are summarized in the Appendix. All channels show a signal yield consistent with the background-only hypothesis. The most significant deviation is seen in the $\Lambda_c^+\pi^+D^-$ channel. The fit result for this channel is shown in Fig. 6. When fitting with the mass and width of the known pentaquark states, the local significance in these spectra is found to be close to (or equal to) zero in all cases and is summarized in Table III.

V. CONCLUSION

Using an integrated luminosity of 5.7 fb^{-1} of pp collision data collected by the LHCb detector, a large range of combinations of open-charm and hidden-charm hadronic states are investigated for possible pentaquark decay channels. A signal model based on the known pentaquark states is also fitted, and the signal yield is found to be consistent with zero in all cases. When scanning the Q-value distribution from threshold to 600 MeV/c^2, the upper limit on the yield relative to the normalization channel is set at 90% and 95% confidence levels. The highest significance is seen in the $\Lambda_c^+\pi^+D^-$ final state; however, using studies of background-only pseudoexperiments this is found to be consistent with the background-only hypothesis.

ACKNOWLEDGMENTS

We express our gratitude to our colleagues in the CERN accelerator departments for the excellent performance of the LHC. We thank the technical and administrative staff at the LHCb institutes. We acknowledge support from CERN and from the national agencies: CAPES, CNPq, FAPERJ, and FINEP (Brazil); MOST and NSFC (China); CNRS/IN2P3 (France); BMBF, DFG, and MPG (Germany); INFN (Italy); NWO (Netherlands); MNiSW and NCN (Poland); MCID/IFA (Romania); MICINN (Spain); SNSF and SER (Switzerland); NASU (Ukraine); STFC (United Kingdom); DOE NP and NSF (USA). We acknowledge the computing resources that are provided by CERN, IN2P3 (France), KIT and DESY (Germany), INFN (Italy), SURF (Netherlands), PIC (Spain), GridPP (United Kingdom), CSCS (Switzerland), IFIN-HH (Romania), CBPF (Brazil), and Polish WLCG (Poland). We are indebted to the communities behind the multiple open-source software packages on which we depend. Individual groups or members have received support from ARC and ARDC (Australia); Key Research Program of Frontier Sciences of CAS, CAS PIFI, CAS CCEPP, Fundamental Research Funds for the Central Universities, and Sci. & Tech. Program of Guangzhou (China); Minciencias (Colombia); EPLANET, Marie Skłodowska-Curie Actions, ERC, and NextGenerationEU (European Union); A*MIDEX, ANR, IPhU, and Labex P2IO, and Région Auvergne-Rhône-Alpes (France); AvH Foundation (Germany); ICSC (Italy); GVA, XuntaGal, GENCAT, Inditex, InTalent, and Prog. Atracción Talento, CM (Spain); SRC (Sweden); the Leverhulme Trust, the Royal Society, and UKRI (United Kingdom).

APPENDIX: SUMMARY TABLES

Tables IV–VI summarize the upper limits set for each signal channel, along with the signal yields with corresponding significances, as well as the Q value that these values occur at.

TABLE IV. Upper limits on $R(\Lambda_c^+)$ at 90% and 95% CL are shown for 11 of the hidden-charm modes, for their lowest p value and highest significance (both local and corrected for LEE) found in the mass scan for all signal models. The Q value and signal yield for these points are also summarized, where the error on the signal yield is statistical only. The Q value can be converted to the absolute mass by adding the masses of each decay product in the respective combination.

Decay mode	Width (MeV/c^2)	Lowest p value Local	Lowest p value Corrected	Significance (σ) Local	Significance (σ) Corrected	Q value (MeV/c^2)	Signal yield	UL ($\times 10^{-3}$) 90% CL	UL ($\times 10^{-3}$) 95% CL
$\Lambda_c^+\ \bar{D}^0$	0	4.7×10^{-3}	0.36	2.60	0.36	353	22.7 ± 30.6	1.41	1.54
	5	3.4×10^{-3}	0.20	2.71	0.86	353	31.4 ± 12.8	1.53	1.64
	10	2.7×10^{-3}	0.13	2.78	1.15	349	39.4 ± 34.8	1.54	1.65
	15	2.2×10^{-3}	0.09	2.85	1.36	349	46.8 ± 91.0	1.57	1.67
$\Lambda_c^+\ D^-$	0	4.7×10^{-3}	0.38	2.60	0.31	501	24.0 ± 12.9	2.05	2.25
	5	3.7×10^{-3}	0.22	2.67	0.77	497	26.7 ± 22.2	2.09	2.27
	10	2.7×10^{-3}	0.13	2.78	1.15	497	33.1 ± 23.0	2.17	2.35
	15	3×10^{-3}	0.11	2.75	1.21	497	38.0 ± 25.5	2.23	2.39
$\Lambda_c^+\ D^{*-}$	0	1.4×10^{-3}	0.12	2.99	1.17	417	17.5 ± 6.9	2.48	2.72
	5	2.2×10^{-3}	0.13	2.85	1.13	417	20.8 ± 9.3	2.74	2.94
	10	3×10^{-3}	0.13	2.75	1.11	421	23.8 ± 9.6	2.80	2.96
	15	4.7×10^{-3}	0.16	2.60	0.99	421	26.3 ± 10.8	2.85	3.00
$\Sigma_c^{++}\ \bar{D}^0$	0	1.2×10^{-3}	0.10	3.04	1.27	301	7.0 ± 3.2	1.10	1.22
	5	4.3×10^{-3}	0.23	2.63	0.73	301	7.7 ± 3.6	1.23	1.37
	10	1.4×10^{-2}	0.48	2.21	0.04	301	7.9 ± 4.1	1.32	1.49
	15	3.2×10^{-2}	0.81	1.85	0.00	301	7.9 ± 4.5	1.40	1.59
$\Lambda_c^+\ \pi^+\ \bar{D}^0$	0	7.4×10^{-4}	0.06	3.18	1.58	245	41.9 ± 13.7	2.87	3.06
	5	9.69×10^{-5}	5.76×10^{-3}	3.73	2.53	245	67.6 ± 19.2	3.22	3.35
	10	2.46×10^{-5}	1.12×10^{-3}	4.06	3.06	245	91.6 ± 24.1	3.29	3.39
	15	8.61×10^{-6}	3.11×10^{-4}	4.30	3.42	245	115.0 ± 28.5	3.30	3.40
$\Sigma_c^{++}\ D^-$	0	5.2×10^{-3}	0.41	2.56	0.24	181	3.9 ± 2.3	1.07	1.21
	5	4.1×10^{-3}	0.22	2.65	0.76	177	6.8 ± 3.3	1.46	1.63
	10	3.7×10^{-3}	0.15	2.68	1.02	177	7.9 ± 3.7	1.64	1.84
	15	4.7×10^{-3}	0.15	2.60	1.03	177	8.4 ± 4.0	1.76	1.98
$\Lambda_c^+\ \pi^+\ D^-$	0	1.6×10^{-4}	0.01	3.59	2.21	225	41.6 ± 12.6	3.95	4.19
	5	3.03×10^{-5}	1.96×10^{-3}	4.01	2.89	225	64.7 ± 17.4	4.43	4.69
	10	8.61×10^{-6}	4.44×10^{-4}	4.30	3.32	225	87.1 ± 21.6	4.64	4.85
	15	3.36×10^{-6}	1.45×10^{-4}	4.50	3.62	225	108.2 ± 25.3	4.72	4.90
$\Lambda_c^+\ \pi^+\ D^{*-}$	0	2.7×10^{-3}	0.20	2.78	0.86	213	12.8 ± 5.3	3.42	3.75
	5	4.5×10^{-4}	0.02	3.32	1.96	213	22.3 ± 7.8	4.52	4.76
	10	1.45×10^{-4}	6.29×10^{-3}	3.62	2.50	213	30.4 ± 9.7	4.75	4.93
	15	7.42×10^{-5}	2.60×10^{-3}	3.79	2.79	209	37.7 ± 11.4	4.85	5.02
$\Sigma_c^0\ \bar{D}^0$	0	1.3×10^{-2}	0.95	2.22	0.00	65	2.9 ± 2.0	0.68	0.78
	5	1.7×10^{-2}	0.79	2.13	0.00	65	3.7 ± 68.8	0.90	1.03
	10	2.2×10^{-2}	0.74	2.02	0.00	65	4.4 ± 4.3	1.02	1.18
	15	2.8×10^{-2}	0.74	1.90	0.00	65	4.8 ± 4.2	1.13	1.29
$\Lambda_c^+\ \pi^-\ \bar{D}^0$	0	4.8×10^{-4}	0.04	3.30	1.72	597	54.0 ± 17.2	2.79	2.98
	5	9.65×10^{-5}	7.11×10^{-3}	3.73	2.45	597	78.8 ± 21.9	3.02	3.20
	10	2.71×10^{-5}	1.63×10^{-3}	4.04	2.94	597	104.0 ± 26.3	3.15	3.30
	15	9.50×10^{-6}	4.83×10^{-4}	4.28	3.30	597	128.5 ± 30.4	3.20	3.33
$\Sigma_c^0\ D^-$	0	2.3×10^{-3}	0.19	2.84	0.88	261	4.4 ± 2.7	1.24	1.39
	5	3.4×10^{-3}	0.18	2.71	0.90	261	5.7 ± 3.0	1.50	1.69
	10	6×10^{-3}	0.23	2.51	0.74	261	6.4 ± 3.4	1.66	1.87
	15	1×10^{-2}	0.30	2.32	0.53	261	7.0 ± 3.8	1.78	2.03

TABLE V. Upper limits on $R(\Lambda_c^+)$ at 90% and 95% CL are shown for eight of the hidden-charm modes, for their lowest p value and highest significance (both local and corrected for LEE) found in the mass scan for all signal models. The Q value and signal yield for these points are also summarized, where the error on the signal yield is statistical only. The Q value can be converted to the absolute mass by adding the masses of each decay product in the respective combination.

Decay mode	Width (MeV)	Lowest p value Local	Corrected	Significance (σ) Local	Corrected	Q value (MeV/c^2)	Signal yield	UL ($\times 10^{-3}$) 90% CL	95% CL
$\Lambda_c^+\ \pi^-\ D^-$	0	3.9×10^{-4}	0.03	3.36	1.90	257	38.1 ± 12.4	4.28	4.56
	5	5.71×10^{-5}	3.33×10^{-3}	3.86	2.71	253	62.1 ± 17.1	4.62	4.83
	10	1.45×10^{-5}	6.92×10^{-4}	4.18	3.20	249	83.7 ± 21.2	4.72	4.88
	15	4.59×10^{-6}	1.83×10^{-4}	4.44	3.56	249	103.5 ± 24.6	4.77	4.92
$\Lambda_c^+\ \pi^-\ D^{*-}$	0	4.4×10^{-3}	0.31	2.62	0.48	197	12.0 ± 5.3	3.11	3.45
	5	7.1×10^{-3}	0.31	2.45	0.51	197	16.8 ± 7.3	4.08	4.53
	10	8.6×10^{-3}	0.27	2.38	0.61	197	21.2 ± 9.1	4.69	5.15
	15	8.9×10^{-3}	0.22	2.37	0.78	197	25.5 ± 10.8	5.11	5.56
$\Sigma_c^{*++}\ \bar{D}^0$	0	1×10^{-2}	0.75	2.32	0.00	37	5.0 ± 2.8	0.96	1.09
	5	1.2×10^{-2}	0.62	2.24	0.00	37	7.8 ± 4.0	1.32	1.49
	10	2.7×10^{-2}	0.92	1.92	0.00	205	7.0 ± 20.6	1.57	1.78
	15	2.7×10^{-2}	0.73	1.92	0.00	485	12.5 ± 6.7	2.23	2.49
$\Sigma_c^{*++}\ D^-$	0	1.2×10^{-3}	0.11	3.03	1.21	537	6.5 ± 3.3	1.63	1.82
	5	1.6×10^{-3}	0.10	2.95	1.30	497	11.8 ± 5.0	2.52	2.79
	10	2.5×10^{-3}	0.11	2.81	1.24	497	13.0 ± 5.7	2.82	3.12
	15	4.3×10^{-3}	0.14	2.63	1.07	497	13.9 ± 6.3	3.02	3.37
$\Sigma_c^{*++}\ D^{*-}$	0	2.3×10^{-2}	1.40	2.00	0.00	193	2.5 ± 1.8	1.08	1.23
	5	3.5×10^{-2}	1.44	1.81	0.00	449	2.9 ± 2.1	1.26	1.45
	10	3.5×10^{-2}	1.08	1.81	0.00	453	3.2 ± 2.3	1.36	1.57
	15	4.1×10^{-2}	0.99	1.74	0.00	453	3.3 ± 2.4	1.45	1.66
$\Sigma_c^{*0}\ \bar{D}^0$	0	3.4×10^{-3}	0.27	2.71	0.63	341	11.4 ± 5.0	1.64	1.83
	5	2.6×10^{-3}	0.14	2.80	1.07	341	16.8 ± 6.8	2.29	2.56
	10	2.2×10^{-3}	0.09	2.84	1.31	341	21.3 ± 8.3	2.73	3.00
	15	1.8×10^{-3}	0.06	2.90	1.52	337	26.0 ± 9.6	3.02	3.27
$\Sigma_c^{*0}\ D^-$	0	7.2×10^{-3}	0.53	2.45	0.00	113	6.2 ± 3.2	1.44	1.62
	5	1.4×10^{-3}	0.08	2.99	1.40	537	11.5 ± 4.8	2.60	2.85
	10	1.1×10^{-3}	0.05	3.06	1.66	537	13.6 ± 5.4	2.99	3.27
	15	1.2×10^{-3}	0.04	3.02	1.70	537	15.1 ± 6.0	3.23	3.54
$\Sigma_c^{*0}\ D^{*-}$	0	9.9×10^{-3}	0.51	2.33	0.00	109	2.6 ± 1.7	0.96	1.11
	5	3.2×10^{-3}	0.16	2.73	0.99	17	2.8 ± 1.9	1.07	1.22
	10	4.1×10^{-3}	0.16	2.64	1.01	17	2.9 ± 2.1	1.13	1.30
	15	3.1×10^{-3}	0.17	2.51	0.94	17	3.0 ± 2.4	1.18	1.34

TABLE VI. Upper limits on $R(\Lambda_c^+)$ at 90% and 95% CL are shown for each doubly charmed mode, for their lowest p value and highest significance (both local and corrected for LEE) found in the mass scan for all signal models. The Q value and signal yield for these points are also summarized, where the error on the signal yield is statistical only. The Q value can be converted to the absolute mass by adding the masses of each decay product in the respective combination.

Decay mode	Width (MeV)	Lowest p value Local	Corrected	Significance (σ) Local	Corrected	Q value (MeV/c^2)	Signal yield	UL ($\times 10^{-3}$) 90% CL	95% CL
$\Lambda_c^+ D^0$	0	8.2×10^{-3}	0.59	2.40	0.00	37	15.0 ± 7.3	0.97	1.06
	5	4.7×10^{-3}	0.26	2.60	0.64	153	26.8 ± 11.0	1.19	1.26
	10	2.7×10^{-3}	0.12	2.78	1.17	153	36.5 ± 14.0	1.27	1.35
	15	2.4×10^{-3}	0.09	2.82	1.34	153	45.0 ± 16.5	1.33	1.43
$\Lambda_c^+ D^+$	0	2×10^{-2}	1.43	2.05	0.00	133	9.4 ± 5.0	1.01	1.13
	5	4.7×10^{-3}	0.27	2.60	0.61	169	11.0 ± 9.9	1.25	1.41
	10	4.2×10^{-3}	0.18	2.64	0.90	169	13.5 ± 24.5	1.52	1.72
	15	5.8×10^{-3}	0.20	2.52	0.85	169	14.9 ± 7.6	1.71	1.92
$\Lambda_c^+ D^{*+}$	0	2.1×10^{-2}	1.25	2.04	0.00	29	3.5 ± 2.3	0.69	0.80
	5	1×10^{-2}	0.49	2.31	0.02	33	6.2 ± 4.2	1.15	1.32
	10	8.1×10^{-3}	0.31	2.41	0.51	33	8.8 ± 5.3	1.45	1.64
	15	7.1×10^{-3}	0.22	2.45	0.76	33	10.5 ± 6.2	1.66	1.88
$\Lambda_c^+ \pi^+ D^0$	0	2.7×10^{-3}	0.22	2.78	0.77	193	18.0 ± 7.2	2.02	2.19
	5	1.6×10^{-3}	0.09	2.95	1.32	193	28.0 ± 10.4	2.32	2.46
	10	1.4×10^{-3}	0.07	2.99	1.51	193	36.7 ± 12.9	2.46	2.62
	15	1.4×10^{-3}	0.05	2.99	1.61	197	44.8 ± 15.3	2.70	2.87
$\Lambda_c^+ \pi^+ D^+$	0	8.7×10^{-3}	0.49	2.38	0.03	225	12.2 ± 5.9	2.04	2.29
	5	2.5×10^{-3}	0.11	2.81	1.23	229	21.8 ± 8.5	3.05	3.32
	10	9.9×10^{-4}	0.03	3.09	1.81	229	29.1 ± 10.3	3.44	3.70
	15	5.9×10^{-4}	0.02	3.25	2.12	229	35.3 ± 11.9	3.70	3.96
$\Lambda_c^+ \pi^+ D^{*+}$	0	5.9×10^{-3}	0.39	2.52	0.28	77	1.9 ± 1.5	0.84	0.95
	5	4.5×10^{-3}	0.22	2.61	0.77	161	6.5 ± 3.6	1.81	2.04
	10	2.9×10^{-3}	0.11	2.76	1.23	161	9.2 ± 4.4	2.31	2.58
	15	1.5×10^{-3}	0.05	2.96	1.64	165	12.2 ± 5.1	2.80	3.10
$\Lambda_c^+ \pi^- D^0$	0	7.3×10^{-4}	0.06	3.18	1.53	593	20.3 ± 7.4	2.11	2.25
	5	6.6×10^{-4}	0.04	3.21	1.78	593	26.3 ± 9.3	2.26	2.38
	10	5.9×10^{-4}	0.03	3.24	1.95	593	32.3 ± 11.0	2.35	2.47
	15	4.8×10^{-4}	0.02	3.30	2.13	593	38.3 ± 12.5	2.42	2.54
$\Lambda_c^+ \pi^- D^+$	0	1.2×10^{-4}	0.01	3.67	2.32	153	21.4 ± 6.9	2.99	3.24
	5	2.07×10^{-5}	1.36×10^{-3}	4.10	3.00	153	33.3 ± 9.5	3.65	3.88
	10	9.44×10^{-6}	4.93×10^{-4}	4.28	3.29	153	43.1 ± 11.6	4.06	4.28
	15	5.96×10^{-6}	2.54×10^{-4}	4.38	3.48	153	51.7 ± 13.4	4.29	4.48
$\Lambda_c^+ \pi^- D^{*+}$	0	2.3×10^{-3}	0.17	2.84	0.97	73	3.2 ± 3.0	1.19	1.35
	5	6.8×10^{-4}	0.04	3.20	1.76	73	5.7 ± 3.3	1.71	1.92
	10	8.5×10^{-4}	0.04	3.14	1.79	73	7.0 ± 3.8	1.94	2.19
	15	1.3×10^{-3}	0.04	3.01	1.70	73	7.6 ± 4.2	2.10	2.36
$\Sigma_c^{*++} D^0$	0	1.2×10^{-2}	0.88	2.27	0.00	113	2.5 ± 1.8	0.63	0.72
	5	9.4×10^{-3}	0.50	2.35	0.00	113	3.2 ± 2.2	0.76	0.87
	10	1.3×10^{-2}	0.48	2.23	0.04	113	3.6 ± 2.4	0.87	1.00
	15	1.8×10^{-2}	0.52	2.11	0.00	113	3.9 ± 2.7	0.95	1.11
$\Sigma_c^{*++} D^+$	0	6×10^{-3}	0.48	2.51	0.05	133	1.9 ± 1.5	0.70	0.81
	5	6.8×10^{-3}	0.37	2.47	0.34	133	2.7 ± 1.9	0.89	1.02
	10	8.8×10^{-3}	0.34	2.37	0.41	133	3.0 ± 2.1	0.97	1.11
	15	1.2×10^{-2}	0.35	2.27	0.38	133	3.2 ± 2.2	1.03	1.18

(Table continued)

TABLE VI. *(Continued)*

Decay mode	Width (MeV)	Lowest p value Local	Lowest p value Corrected	Significance (σ) Local	Significance (σ) Corrected	Q value (MeV$/c^2$)	Signal yield	UL ($\times 10^{-3}$) 90% CL	UL ($\times 10^{-3}$) 95% CL
$\Sigma_c^{*0}\ D^0$	0	1.52×10^{-5}	1.67×10^{-3}	4.17	2.93	89	3.9 ± 2.0	0.68	0.76
	5	5.13×10^{-5}	3.70×10^{-3}	3.88	2.68	89	5.3 ± 2.6	0.90	0.99
	10	1.06×10^{-4}	5.47×10^{-3}	3.70	2.54	89	6.2 ± 3.0	1.03	1.14
	15	1.66×10^{-4}	6.69×10^{-3}	3.59	2.47	89	6.8 ± 3.2	1.13	1.25
$\Sigma_c^{*0}\ D^+$	0	1.8×10^{-2}	1.20	2.10	0.00	325	2.6 ± 1.8	0.88	1.01
	5	1.3×10^{-2}	0.61	2.23	0.00	73	3.5 ± 2.4	1.12	1.29
	10	1.3×10^{-2}	0.48	2.21	0.06	73	3.8 ± 3.2	1.29	1.50
	15	1.5×10^{-2}	0.41	2.18	0.22	69	4.7 ± 3.7	1.51	1.75

[1] M. Gell-Mann, A schematic model of baryons and mesons, Phys. Lett. **8**, 214 (1964).

[2] G. Zweig, in *An SU(3) Model for Strong Interaction Symmetry and its Breaking. Version 2*, edited by D. B. Lichtenberg and S. P. Rosen (1964), pp. 22–101, 10.17181/CERN-TH-412.

[3] R. L. Jaffe, Perhaps a stable dihyperon, Phys. Rev. Lett. **38**, 195 (1977); Phys. Rev. Lett. **38**, 617(E) (1977).

[4] D. Horn and J. Mandula, A model of mesons with constituent gluons, Phys. Rev. D **17**, 898 (1978).

[5] H. Fritzsch, M. Gell-Mann, and H. Leutwyler, Advantages of the color octet gluon picture, Phys. Lett. **47B**, 365 (1973).

[6] B. Aubert *et al.* (*BABAR* Collaboration), Observation of a narrow meson decaying to $D_s^+\pi^0$ at a mass of 2.32 GeV$/c^2$, Phys. Rev. Lett. **90**, 242001 (2003).

[7] S. K. Choi *et al.* (Belle Collaboration), Observation of a narrow charmonium-like state in exclusive $B^\pm \to K^\pm\pi^+\pi^- J/\psi$ decays, Phys. Rev. Lett. **91**, 262001 (2003).

[8] S. K. Choi *et al.* (Belle Collaboration), Observation of a resonance-like structure in the $\pi^\pm\psi'$ mass distribution in exclusive $B \to K\pi^\pm\psi'$ decays, Phys. Rev. Lett. **100**, 142001 (2008).

[9] R. Aaij *et al.* (LHCb Collaboration), Observation of $J/\psi p$ resonances consistent with pentaquark states in $\Lambda_b^0 \to J/\psi pK^-$ decays, Phys. Rev. Lett. **115**, 072001 (2015).

[10] R. Aaij *et al.* (LHCb Collaboration), Model-independent evidence for $J/\psi p$ contributions to $\Lambda_b^0 \to J/\psi pK^-$ decays, Phys. Rev. Lett. **117**, 082002 (2016).

[11] R. Aaij *et al.* (LHCb Collaboration), Observation of a narrow pentaquark state, $P_c(4312)^+$, and of two-peak structure of the $P_c(4450)^+$, Phys. Rev. Lett. **122**, 222001 (2019).

[12] R. Aaij *et al.* (LHCb Collaboration), Observation of an exotic narrow doubly charmed tetraquark, Nat. Phys. **18**, 751 (2022).

[13] R. Aaij *et al.* (LHCb Collaboration), Study of the doubly charmed tetraquark T_{cc}^+, Nat. Commun. **13**, 3351 (2022).

[14] F. E. Close and P. R. Page, The $D^{*0}\bar{D}^0$ threshold resonance, Phys. Lett. B **578**, 119 (2004).

[15] M. Karliner and J. L. Rosner, New exotic meson and baryon resonances from doubly-heavy hadronic molecules, Phys. Rev. Lett. **115**, 122001 (2015).

[16] L. Maiani, F. Piccinini, A. D. Polosa, and V. Riquer, Diquark-antidiquarks with hidden or open charm and the nature of $X(3872)$, Phys. Rev. D **71**, 014028 (2005).

[17] L. Maiani, A. D. Polosa, and V. Riquer, The new pentaquarks in the diquark model, Phys. Lett. B **749**, 289 (2015).

[18] S. Dubynskiy and M. B. Voloshin, Hadro-charmonium, Phys. Lett. B **666**, 344 (2008).

[19] D. V. Bugg, An explanation of Belle states $Z_b(10610)$ and $Z_b(10650)$, Europhys. Lett. **96**, 11002 (2011).

[20] P. Pakhlov and T. Uglov, Charged charmonium-like $Z^+(4430)$ from rescattering in conventional B decays, Phys. Lett. B **748**, 183 (2015).

[21] G. Yang, J. Ping, and J. Segovia, Doubly charmed pentaquarks, Phys. Rev. D **101**, 074030 (2020).

[22] M. Padmanath, R. G. Edwards, N. Mathur, and M. Peardon, Spectroscopy of doubly and triply-charmed baryons from lattice QCD, *Proc. Sci.*, LATTICE2013 (2014) 247 [arXiv:1311.4354].

[23] A. A. Alves Jr. *et al.* (LHCb Collaboration), The LHCb detector at the LHC, J. Instrum. **3**, S08005 (2008).

[24] R. Aaij *et al.* (LHCb Collaboration), LHCb detector performance, Int. J. Mod. Phys. A **30**, 1530022 (2015).

[25] R. Aaij *et al.*, Performance of the LHCb trigger and full real-time reconstruction in Run 2 of the LHC, J. Instrum. **14**, P04013 (2019).

[26] S. Borghi, Novel real-time alignment and calibration of the LHCb detector and its performance, Nucl. Instrum. Methods Phys. Res., Sect. A **845**, 560 (2017).

[27] R. Aaij *et al.*, The LHCb trigger and its performance in 2011, J. Instrum. **8**, P04022 (2013).

[28] R. Aaij *et al.*, Tesla: An application for real-time data analysis in high energy physics, Comput. Phys. Commun. **208**, 35 (2016).

[29] T. Sjöstrand, S. Mrenna, and P. Skands, PYTHIA 6.4 physics and manual, J. High Energy Phys. 05 (2006) 026; A brief introduction to PYTHIA 8.1, Comput. Phys. Commun. **178**, 852 (2008).

[30] I. Belyaev *et al.*, Handling of the generation of primary events in Gauss, the LHCb simulation framework, J. Phys. Conf. Ser. **331**, 032047 (2011).
[31] D. J. Lange, The EvtGen particle decay simulation package, Nucl. Instrum. Methods Phys. Res., Sect. A **462**, 152 (2001).
[32] P. Golonka and Z. Was, PHOTOS Monte Carlo: A precision tool for QED corrections in Z and W decays, Eur. Phys. J. C **45**, 97 (2006).
[33] J. Allison *et al.* (GEANT4 Collaboration), GEANT4 developments and applications, IEEE Trans. Nucl. Sci. **53**, 270 (2006); S. Agostinelli *et al.* (GEANT4 Collaboration), GEANT4: A simulation toolkit, Nucl. Instrum. Methods Phys. Res., Sect. A **506**, 250 (2003).
[34] M. Clemencic, G. Corti, S. Easo, C. R. Jones, S. Miglioranzi, M. Pappagallo, and P. Robbe, The LHCb simulation application, Gauss: Design, evolution and experience, J. Phys. Conf. Ser. **331**, 032023 (2011).
[35] R. Aaij *et al.* (LHCb Collaboration), Observation of new Ξ_c^0 baryons decaying to $\Lambda_c^+ K^-$, Phys. Rev. Lett. **124**, 222001 (2020).
[36] A. Hoecker *et al.*, TMVA 4—Toolkit for multivariate data analysis with ROOT. Users Guide, arXiv:physics/0703039.
[37] T. Skwarnicki, A study of the radiative cascade transitions between the Upsilon-prime and Upsilon resonances, Ph.D. thesis, Institute of Nuclear Physics, Krakow, 1986.
[38] E. Gross and O. Vitells, Trial factors for the look elsewhere effect in high energy physics, Eur. Phys. J. C **70**, 525 (2010).
[39] R. L. Workman *et al.* (Particle Data Group), Review of particle physics, Prog. Theor. Exp. Phys. **2022**, 083C01 (2022).

R. Aaij,[33] A. S. W. Abdelmotteleb,[52] C. Abellan Beteta,[46] F. Abudinén,[52] T. Ackernley,[56] B. Adeva,[42] M. Adinolfi,[50] P. Adlarson,[78] H. Afsharnia,[10] C. Agapopoulou,[44] C. A. Aidala,[79] Z. Ajaltouni,[10] S. Akar,[61] K. Akiba,[33] P. Albicocco,[24] J. Albrecht,[16] F. Alessio,[44] M. Alexander,[55] A. Alfonso Albero,[41] Z. Aliouche,[58] P. Alvarez Cartelle,[51] R. Amalric,[14] S. Amato,[2] J. L. Amey,[50] Y. Amhis,[12,44] L. An,[5] L. Anderlini,[23] M. Andersson,[46] A. Andreianov,[39] P. Andreola,[46] M. Andreotti,[22] D. Andreou,[64] D. Ao,[6] F. Archilli,[32,b] S. Arguedas Cuendis,[8] A. Artamonov,[39] M. Artuso,[64] E. Aslanides,[11] M. Atzeni,[60] B. Audurier,[13] D. Bacher,[59] I. Bachiller Perea,[9] S. Bachmann,[18] M. Bachmayer,[45] J. J. Back,[52] A. Bailly-reyre,[14] P. Baladron Rodriguez,[42] V. Balagura,[13] W. Baldini,[22,44] J. Baptista de Souza Leite,[1] M. Barbetti,[23,c] I. R. Barbosa,[66] R. J. Barlow,[58] S. Barsuk,[12] W. Barter,[54] M. Bartolini,[51] F. Baryshnikov,[39] J. M. Basels,[15] G. Bassi,[30,d] B. Batsukh,[4] A. Battig,[16] A. Bay,[45] A. Beck,[52] M. Becker,[16] F. Bedeschi,[30] I. B. Bediaga,[1] A. Beiter,[64] S. Belin,[42] V. Bellee,[46] K. Belous,[39] I. Belov,[25] I. Belyaev,[39] G. Benane,[11] G. Bencivenni,[24] E. Ben-Haim,[14] A. Berezhnoy,[39] R. Bernet,[46] S. Bernet Andres,[40] D. Berninghoff,[18] H. C. Bernstein,[64] C. Bertella,[58] A. Bertolin,[29] C. Betancourt,[46] F. Betti,[54] J. Bex,[51] Ia. Bezshyiko,[46] J. Bhom,[36] L. Bian,[70] M. S. Bieker,[16] N. V. Biesuz,[22] P. Billoir,[14] A. Biolchini,[33] M. Birch,[57] F. C. R. Bishop,[51] A. Bitadze,[58] A. Bizzeti, M. P. Blago,[51] T. Blake,[52] F. Blanc,[45] J. E. Blank,[16] S. Blusk,[64] D. Bobulska,[55] V. Bocharnikov,[39] J. A. Boelhauve,[16] O. Boente Garcia,[13] T. Boettcher,[61] A. Bohare,[54] A. Boldyrev,[39] C. S. Bolognani,[76] R. Bolzonella,[22,e] N. Bondar,[39] F. Borgato,[29,44,f] S. Borghi,[58] M. Borsato,[18] J. T. Borsuk,[36] S. A. Bouchiba,[45] T. J. V. Bowcock,[56] A. Boyer,[44] C. Bozzi,[22] M. J. Bradley,[57] S. Braun,[62] A. Brea Rodriguez,[42] N. Breer,[16] J. Brodzicka,[36] A. Brossa Gonzalo,[42] J. Brown,[56] D. Brundu,[28] A. Buonaura,[46] L. Buonincontri,[29,f] A. T. Burke,[58] C. Burr,[44] A. Bursche,[68] A. Butkevich,[39] J. S. Butter,[33] J. Buytaert,[44] W. Byczynski,[44] S. Cadeddu,[28] H. Cai,[70] R. Calabrese,[22,e] L. Calefice,[16] S. Cali,[24] M. Calvi,[27,g] M. Calvo Gomez,[40] J. I. Cambon Bouzas,[42] P. Campana,[24] D. H. Campora Perez,[76] A. F. Campoverde Quezada,[6] S. Capelli,[27,g] L. Capriotti,[22] A. Carbone,[21,h] L. Carcedo Salgado,[42] R. Cardinale,[25,i] A. Cardini,[28] P. Carniti,[27,g] L. Carus,[18] A. Casais Vidal,[42] R. Caspary,[18] G. Casse,[56] M. Cattaneo,[44] G. Cavallero,[22] V. Cavallini,[22,e] S. Celani,[45] J. Cerasoli,[11] D. Cervenkov,[59] S. Cesare,[26,j] A. J. Chadwick,[56] I. Chahrour,[79] M. G. Chapman,[50] M. Charles,[14] Ph. Charpentier,[44] C. A. Chavez Barajas,[56] M. Chefdeville,[9] C. Chen,[11] S. Chen,[4] A. Chernov,[36] S. Chernyshenko,[48] V. Chobanova,[42,k] S. Cholak,[45] M. Chrzaszcz,[36] A. Chubykin,[39] V. Chulikov,[39] P. Ciambrone,[24] M. F. Cicala,[52] X. Cid Vidal,[42] G. Ciezarek,[44] P. Cifra,[44] P. E. L. Clarke,[54] M. Clemencic,[44] H. V. Cliff,[51] J. Closier,[44] J. L. Cobbledick,[58] C. Cocha Toapaxi,[18] V. Coco,[44] J. Cogan,[11] E. Cogneras,[10] L. Cojocariu,[38] P. Collins,[44] T. Colombo,[44] A. Comerma-Montells,[41] L. Congedo,[20] A. Contu,[28] N. Cooke,[55] I. Corredoira,[42] A. Correia,[14] G. Corti,[44] J. J. Cottee Meldrum,[50] B. Couturier,[44] D. C. Craik,[46] M. Cruz Torres,[1,l] R. Currie,[54] C. L. Da Silva,[63] S. Dadabaev,[39] L. Dai,[67] X. Dai,[5] E. Dall'Occo,[16] J. Dalseno,[42] C. D'Ambrosio,[44] J. Daniel,[10] A. Danilina,[39] P. d'Argent,[20] A. Davidson,[52] J. E. Davies,[58] A. Davis,[58] O. De Aguiar Francisco,[58] C. De Angelis,[28,m] J. de Boer,[33]

K. De Bruyn,[75] S. De Capua,[58] M. De Cian,[18] U. De Freitas Carneiro Da Graca,[1,n] E. De Lucia,[24] J. M. De Miranda,[1] L. De Paula,[2] M. De Serio,[20,o] D. De Simone,[46] P. De Simone,[24] F. De Vellis,[16] J. A. de Vries,[76] C. T. Dean,[63] F. Debernardis,[20,o] D. Decamp,[9] V. Dedu,[11] L. Del Buono,[14] B. Delaney,[60] H.-P. Dembinski,[16] J. Deng,[7] V. Denysenko,[46] O. Deschamps,[10] F. Dettori,[28,m] B. Dey,[73] P. Di Nezza,[24] I. Diachkov,[39] S. Didenko,[39] S. Ding,[64] V. Dobishuk,[48] A. D. Docheva,[55] A. Dolmatov,[39] C. Dong,[3] A. M. Donohoe,[19] F. Dordei,[28] A. C. dos Reis,[1] L. Douglas,[55] A. G. Downes,[9] W. Duan,[68] P. Duda,[77] M. W. Dudek,[36] L. Dufour,[44] V. Duk,[74] P. Durante,[44] M. M. Duras,[77] J. M. Durham,[63] D. Dutta,[58] A. Dziurda,[36] A. Dzyuba,[39] S. Easo,[53,44] E. Eckstein,[72] U. Egede,[65] A. Egorychev,[39] V. Egorychev,[39] C. Eirea Orro,[42] S. Eisenhardt,[54] E. Ejopu,[58] S. Ek-In,[45] L. Eklund,[78] M. Elashri,[61] J. Ellbracht,[16] S. Ely,[57] A. Ene,[38] E. Epple,[61] S. Escher,[15] J. Eschle,[46] S. Esen,[46] T. Evans,[58] F. Fabiano,[28,44,m] L. N. Falcao,[1] Y. Fan,[6] B. Fang,[70,12] L. Fantini,[74,p] M. Faria,[45] K. Farmer,[54] S. Farry,[56] D. Fazzini,[27,g] L. Felkowski,[77] M. Feng,[4,6] M. Feo,[44] M. Fernandez Gomez,[42] A. D. Fernez,[62] F. Ferrari,[21] L. Ferreira Lopes,[45] F. Ferreira Rodrigues,[2] S. Ferreres Sole,[33] M. Ferrillo,[46] M. Ferro-Luzzi,[44] S. Filippov,[39] R. A. Fini,[20] M. Fiorini,[22,e] M. Firlej,[35] K. M. Fischer,[59] D. S. Fitzgerald,[79] C. Fitzpatrick,[58] T. Fiutowski,[35] F. Fleuret,[13] M. Fontana,[21] F. Fontanelli,[25,i] L. F. Foreman,[58] R. Forty,[44] D. Foulds-Holt,[51] M. Franco Sevilla,[62] M. Frank,[44] E. Franzoso,[22,e] G. Frau,[18] C. Frei,[44] D. A. Friday,[58] L. Frontini,[26] J. Fu,[6] Q. Fuehring,[16] Y. Fujii,[65] T. Fulghesu,[14] E. Gabriel,[33] G. Galati,[20,o] M. D. Galati,[33] A. Gallas Torreira,[42] D. Galli,[21,h] S. Gambetta,[54,44] M. Gandelman,[2] P. Gandini,[26] H. Gao,[6] R. Gao,[59] Y. Gao,[7] Y. Gao,[5] Y. Gao,[7] M. Garau,[28,m] L. M. Garcia Martin,[45] P. Garcia Moreno,[41] J. García Pardiñas,[44] B. Garcia Plana,[42] F. A. Garcia Rosales,[13] L. Garrido,[41] C. Gaspar,[44] R. E. Geertsema,[33] L. L. Gerken,[16] E. Gersabeck,[58] M. Gersabeck,[58] T. Gershon,[52] Z. Ghorbanimoghaddam,[50] L. Giambastiani,[29,f] F. I. Giasemis,[14,q] V. Gibson,[51] H. K. Giemza,[37] A. L. Gilman,[59] M. Giovannetti,[24] A. Gioventù,[42] P. Gironella Gironell,[41] C. Giugliano,[22,e] M. A. Giza,[36] K. Gizdov,[54] E. L. Gkougkousis,[44] F. C. Glaser,[12,18] V. V. Gligorov,[14] C. Göbel,[66] E. Golobardes,[40] D. Golubkov,[39] A. Golutvin,[57,39,44] A. Gomes,[1,2,a,r,s] S. Gomez Fernandez,[41] F. Goncalves Abrantes,[59] M. Goncerz,[36] G. Gong,[3] J. A. Gooding,[16] I. V. Gorelov,[39] C. Gotti,[27] J. P. Grabowski,[72] L. A. Granado Cardoso,[44] E. Graugés,[41] E. Graverini,[45] L. Grazette,[52] G. Graziani, A. T. Grecu,[38] L. M. Greeven,[33] N. A. Grieser,[61] L. Grillo,[55] S. Gromov,[39] C. Gu,[13] M. Guarise,[22] M. Guittiere,[12] V. Guliaeva,[39] P. A. Günther,[18] A.-K. Guseinov,[39] E. Gushchin,[39] Y. Guz,[5,39,44] T. Gys,[44] T. Hadavizadeh,[65] C. Hadjivasiliou,[62] G. Haefeli,[45] C. Haen,[44] J. Haimberger,[44] S. C. Haines,[51] M. Hajheidari,[44] T. Halewood-leagas,[56] M. M. Halvorsen,[44] P. M. Hamilton,[62] J. Hammerich,[56] Q. Han,[7] X. Han,[18] S. Hansmann-Menzemer,[18] L. Hao,[6] N. Harnew,[59] T. Harrison,[56] M. Hartmann,[12] C. Hasse,[44] M. Hatch,[44] J. He,[6,t] K. Heijhoff,[33] F. Hemmer,[44] C. Henderson,[61] R. D. L. Henderson,[65,52] A. M. Hennequin,[44] K. Hennessy,[56] L. Henry,[45] J. Herd,[57] J. Heuel,[15] A. Hicheur,[2] D. Hill,[45] M. Hilton,[58] S. E. Hollitt,[16] J. Horswill,[58] R. Hou,[7] Y. Hou,[9] N. Howarth,[56] J. Hu,[18] J. Hu,[68] W. Hu,[5] X. Hu,[3] W. Huang,[6] X. Huang,[70] W. Hulsbergen,[33] R. J. Hunter,[52] M. Hushchyn,[39] D. Hutchcroft,[56] P. Ibis,[16] M. Idzik,[35] D. Ilin,[39] P. Ilten,[61] A. Inglessi,[39] A. Iniukhin,[39] A. Ishteev,[39] K. Ivshin,[39] R. Jacobsson,[44] H. Jage,[15] S. J. Jaimes Elles,[43,71] S. Jakobsen,[44] E. Jans,[33] B. K. Jashal,[43] A. Jawahery,[62] V. Jevtic,[16] E. Jiang,[62] X. Jiang,[4,6] Y. Jiang,[6] Y. J. Jiang,[5] M. John,[59] D. Johnson,[49] C. R. Jones,[51] T. P. Jones,[52] S. Joshi,[37] B. Jost,[44] N. Jurik,[44] I. Juszczak,[36] D. Kaminaris,[45] S. Kandybei,[47] Y. Kang,[3] M. Karacson,[44] D. Karpenkov,[39] M. Karpov,[39] A. Kauniskangas,[45] J. W. Kautz,[61] F. Keizer,[44] D. M. Keller,[64] M. Kenzie,[51] T. Ketel,[33] B. Khanji,[64] A. Kharisova,[39] S. Kholodenko,[30] G. Khreich,[12] T. Kirn,[15] V. S. Kirsebom,[45] O. Kitouni,[60] S. Klaver,[34] N. Kleijne,[30,d] K. Klimaszewski,[37] M. R. Kmiec,[37] S. Koliiev,[48] L. Kolk,[16] A. Konoplyannikov,[39] P. Kopciewicz,[35,44] R. Kopecna,[18] P. Koppenburg,[33] M. Korolev,[39] I. Kostiuk,[33] O. Kot,[48] S. Kotriakhova, A. Kozachuk,[39] P. Kravchenko,[39] L. Kravchuk,[39] M. Kreps,[52] S. Kretzschmar,[15] P. Krokovny,[39] W. Krupa,[64] W. Krzemien,[37] J. Kubat,[18] S. Kubis,[77] W. Kucewicz,[36] M. Kucharczyk,[36] V. Kudryavtsev,[39] E. Kulikova,[39] A. Kupsc,[78] B. K. Kutsenko,[11] D. Lacarrere,[44] G. Lafferty,[58] A. Lai,[28] A. Lampis,[28,m] D. Lancierini,[46] C. Landesa Gomez,[42] J. J. Lane,[65] R. Lane,[50] C. Langenbruch,[18] J. Langer,[16] O. Lantwin,[39] T. Latham,[52] F. Lazzari,[30,u] C. Lazzeroni,[49] R. Le Gac,[11] S. H. Lee,[79] R. Lefèvre,[10] A. Leflat,[39] S. Legotin,[39] O. Leroy,[11] T. Lesiak,[36] B. Leverington,[18] A. Li,[3] H. Li,[68] K. Li,[7] L. Li,[58] P. Li,[44] P.-R. Li,[69] S. Li,[7] T. Li,[4] T. Li,[68] Y. Li,[7] Y. Li,[4] Z. Li,[64] Z. Lian,[3] X. Liang,[64] C. Lin,[6] T. Lin,[53] R. Lindner,[44] V. Lisovskyi,[45] R. Litvinov,[28,m]

G. Liu,[68] H. Liu,[6] K. Liu,[69] Q. Liu,[6] S. Liu,[4,6] Y. Liu,[54] Y. Liu,[69] A. Lobo Salvia,[41] A. Loi,[28]
J. Lomba Castro,[42] T. Long,[51] I. Longstaff,[55] J. H. Lopes,[2] A. Lopez Huertas,[41] S. López Soliño,[42] G. H. Lovell,[51]
Y. Lu,[4,v] C. Lucarelli,[23,c] D. Lucchesi,[29,f] S. Luchuk,[39] M. Lucio Martinez,[76] V. Lukashenko,[33,48] Y. Luo,[3]
A. Lupato,[29] E. Luppi,[22,e] K. Lynch,[19] X.-R. Lyu,[6] G. M. Ma,[3] R. Ma,[6] S. Maccolini,[16] F. Machefert,[12]
F. Maciuc,[38] I. Mackay,[59] L. R. Madhan Mohan,[51] M. M. Madurai,[49] A. Maevskiy,[39] D. Magdalinski,[33]
D. Maisuzenko,[39] M. W. Majewski,[35] J. J. Malczewski,[36] S. Malde,[59] B. Malecki,[36,44] L. Malentacca,[44]
A. Malinin,[39] T. Maltsev,[39] G. Manca,[28,m] G. Mancinelli,[11] C. Mancuso,[26,12,j] R. Manera Escalero,[41]
D. Manuzzi,[21] D. Marangotto,[26,j] J. F. Marchand,[9] U. Marconi,[21] S. Mariani,[44] C. Marin Benito,[41,44] J. Marks,[18]
A. M. Marshall,[50] P. J. Marshall,[56] G. Martelli,[74,p] G. Martellotti,[31] L. Martinazzoli,[44] M. Martinelli,[27,g]
D. Martinez Santos,[42] F. Martinez Vidal,[43] A. Massafferri,[1] M. Materok,[15] R. Matev,[44] A. Mathad,[46]
V. Matiunin,[39] C. Matteuzzi,[64,27] K. R. Mattioli,[13] A. Mauri,[57] E. Maurice,[13] J. Mauricio,[41] M. Mazurek,[44]
M. McCann,[57] L. Mcconnell,[19] T. H. McGrath,[58] N. T. McHugh,[55] A. McNab,[58] R. McNulty,[19] B. Meadows,[61]
G. Meier,[16] D. Melnychuk,[37] M. Merk,[33,76] A. Merli,[26,j] L. Meyer Garcia,[2] D. Miao,[4,6] H. Miao,[6]
M. Mikhasenko,[72,w] D. A. Milanes,[71] A. Minotti,[27,g] E. Minucci,[64] T. Miralles,[10] S. E. Mitchell,[54]
B. Mitreska,[16] D. S. Mitzel,[16] A. Modak,[53] A. Mödden,[16] R. A. Mohammed,[59] R. D. Moise,[15] S. Mokhnenko,[39]
T. Mombächer,[44] M. Monk,[52,65] I. A. Monroy,[71] S. Monteil,[10] A. Morcillo Gomez,[42] G. Morello,[24]
M. J. Morello,[30,d] M. P. Morgenthaler,[18] J. Moron,[35] A. B. Morris,[44] A. G. Morris,[11] R. Mountain,[64] H. Mu,[3]
Z. M. Mu,[5] E. Muhammad,[52] F. Muheim,[54] M. Mulder,[75] K. Müller,[46] F. Muñoz-Rojas,[8] R. Murta,[57]
P. Naik,[56] T. Nakada,[45] R. Nandakumar,[53] T. Nanut,[44] I. Nasteva,[2] M. Needham,[54] N. Neri,[26,j] S. Neubert,[72]
N. Neufeld,[44] P. Neustroev,[39] R. Newcombe,[57] J. Nicolini,[16,12] D. Nicotra,[76] E. M. Niel,[45] N. Nikitin,[39] P. Nogga,[72]
N. S. Nolte,[60] C. Normand,[9,28,m] J. Novoa Fernandez,[42] G. Nowak,[61] C. Nunez,[79] H. N. Nur,[55]
A. Oblakowska-Mucha,[35] V. Obraztsov,[39] T. Oeser,[15] S. Okamura,[22,44,e] A. Okhotnikov,[39] R. Oldeman,[28,m]
F. Oliva,[54] M. Olocco,[16] C. J. G. Onderwater,[76] R. H. O'Neil,[54] J. M. Otalora Goicochea,[2] T. Ovsiannikova,[39]
P. Owen,[46] A. Oyanguren,[43] O. Ozcelik,[54] K. O. Padeken,[72] B. Pagare,[52] P. R. Pais,[18] T. Pajero,[59] A. Palano,[20]
M. Palutan,[24] G. Panshin,[39] L. Paolucci,[52] A. Papanestis,[53] M. Pappagallo,[20,o] L. L. Pappalardo,[22,e]
C. Pappenheimer,[61] C. Parkes,[58,44] B. Passalacqua,[22,e] G. Passaleva,[23] D. Passaro,[30,d] A. Pastore,[20] M. Patel,[57]
J. Patoc,[59] C. Patrignani,[21,h] C. J. Pawley,[76] A. Pellegrino,[33] M. Pepe Altarelli,[24] S. Perazzini,[21] D. Pereima,[39]
A. Pereiro Castro,[42] P. Perret,[10] A. Perro,[44] K. Petridis,[50] A. Petrolini,[25,i] S. Petrucci,[54] H. Pham,[64] L. Pica,[30,d]
M. Piccini,[74] B. Pietrzyk,[9] G. Pietrzyk,[12] D. Pinci,[31] F. Pisani,[44] M. Pizzichemi,[27,g] V. Placinta,[38]
M. Plo Casasus,[42] F. Polci,[14,44] M. Poli Lener,[24] A. Poluektov,[11] N. Polukhina,[39] I. Polyakov,[44] E. Polycarpo,[2]
S. Ponce,[44] D. Popov,[6] S. Poslavskii,[39] K. Prasanth,[36] L. Promberger,[18] C. Prouve,[42] V. Pugatch,[48] V. Puill,[12]
G. Punzi,[30,u] H. R. Qi,[3] W. Qian,[6] N. Qin,[3] S. Qu,[3] R. Quagliani,[45] B. Rachwal,[35] J. H. Rademacker,[50]
M. Rama,[30] M. Ramírez García,[79] M. Ramos Pernas,[52] M. S. Rangel,[2] F. Ratnikov,[39] G. Raven,[34]
M. Rebollo De Miguel,[43] F. Redi,[44] J. Reich,[50] F. Reiss,[58] Z. Ren,[3] P. K. Resmi,[59] R. Ribatti,[30,d]
G. R. Ricart,[13,80] D. Riccardi,[30,d] S. Ricciardi,[53] K. Richardson,[60] M. Richardson-Slipper,[54] K. Rinnert,[56]
P. Robbe,[12] G. Robertson,[54] E. Rodrigues,[56,44] E. Rodriguez Fernandez,[42] J. A. Rodriguez Lopez,[71]
E. Rodriguez Rodriguez,[42] A. Rogovskiy,[53] D. L. Rolf,[44] A. Rollings,[59] P. Roloff,[44] V. Romanovskiy,[39]
M. Romero Lamas,[42] A. Romero Vidal,[42] G. Romolini,[22] F. Ronchetti,[45] M. Rotondo,[24] S. R. Roy,[18]
M. S. Rudolph,[64] T. Ruf,[44] R. A. Ruiz Fernandez,[42] J. Ruiz Vidal,[43] A. Ryzhikov,[39] J. Ryzka,[35]
J. J. Saborido Silva,[42] N. Sagidova,[39] N. Sahoo,[49] B. Saitta,[28,m] M. Salomoni,[44] C. Sanchez Gras,[33]
I. Sanderswood,[43] R. Santacesaria,[31] C. Santamarina Rios,[42] M. Santimaria,[24] L. Santoro,[1] E. Santovetti,[32]
D. Saranin,[39] G. Sarpis,[54] M. Sarpis,[72] A. Sarti,[31] C. Satriano,[31,x] A. Satta,[32] M. Saur,[5] D. Savrina,[39]
H. Sazak,[10] L. G. Scantlebury Smead,[59] A. Scarabotto,[14] S. Schael,[15] S. Scherl,[56] A. M. Schertz,[73]
M. Schiller,[55] H. Schindler,[44] M. Schmelling,[17] B. Schmidt,[44] S. Schmitt,[15] H. Schmitz,[72] O. Schneider,[45]
A. Schopper,[44] N. Schulte,[16] S. Schulte,[45] M. H. Schune,[12] R. Schwemmer,[44] G. Schwering,[15] B. Sciascia,[24]
A. Sciuccati,[44] S. Sellam,[42] A. Semennikov,[39] M. Senghi Soares,[34] A. Sergi,[25,i] N. Serra,[46,44] L. Sestini,[29]
A. Seuthe,[16] Y. Shang,[5] D. M. Shangase,[79] M. Shapkin,[39] I. Shchemerov,[39] L. Shchutska,[45] T. Shears,[56]
L. Shekhtman,[39] Z. Shen,[5] S. Sheng,[4,6] V. Shevchenko,[39] B. Shi,[6] E. B. Shields,[27,g] Y. Shimizu,[12]
E. Shmanin,[39] R. Shorkin,[39] J. D. Shupperd,[64] B. G. Siddi,[22,e] R. Silva Coutinho,[64] G. Simi,[29,f] S. Simone,[20,o]

M. Singla,[65] N. Skidmore,[58] R. Skuza,[18] T. Skwarnicki,[64] M. W. Slater,[49] J. C. Smallwood,[59] J. G. Smeaton,[51] E. Smith,[60] K. Smith,[63] M. Smith,[57] A. Snoch,[33] L. Soares Lavra,[54] M. D. Sokoloff,[61] F. J. P. Soler,[55] A. Solomin,[39,50] A. Solovev,[39] I. Solovyev,[39] R. Song,[65] Y. Song,[45] Y. Song,[3] Y. S. Song,[5] F. L. Souza De Almeida,[2] B. Souza De Paula,[2] E. Spadaro Norella,[26,j] E. Spedicato,[21] J. G. Speer,[16] E. Spiridenkov,[39] P. Spradlin,[55] V. Sriskaran,[44] F. Stagni,[44] M. Stahl,[44] S. Stahl,[44] S. Stanislaus,[59] E. N. Stein,[44] O. Steinkamp,[46] O. Stenyakin,[39] H. Stevens,[16] D. Strekalina,[39] Y. Su,[6] F. Suljik,[59] J. Sun,[28] L. Sun,[70] Y. Sun,[62] P. N. Swallow,[49] K. Swientek,[35] F. Swystun,[52] A. Szabelski,[37] T. Szumlak,[35] M. Szymanski,[44] Y. Tan,[3] S. Taneja,[58] M. D. Tat,[59] A. Terentev,[46] F. Terzuoli,[30,y] F. Teubert,[44] E. Thomas,[44] D. J. D. Thompson,[49] H. Tilquin,[57] V. Tisserand,[10] S. T'Jampens,[9] M. Tobin,[4] L. Tomassetti,[22,e] G. Tonani,[26,j] X. Tong,[5] D. Torres Machado,[1] L. Toscano,[16] D. Y. Tou,[3] C. Trippl,[40] G. Tuci,[18] N. Tuning,[33] L. H. Uecker,[18] A. Ukleja,[37] D. J. Unverzagt,[18] E. Ursov,[39] A. Usachov,[34] A. Ustyuzhanin,[39] U. Uwer,[18] V. Vagnoni,[21] A. Valassi,[44] G. Valenti,[21] N. Valls Canudas,[40] M. Van Dijk,[45] H. Van Hecke,[63] E. van Herwijnen,[57] C. B. Van Hulse,[42,z] R. Van Laak,[45] M. van Veghel,[33] R. Vazquez Gomez,[41] P. Vazquez Regueiro,[42] C. Vázquez Sierra,[42] S. Vecchi,[22] J. J. Velthuis,[50] M. Veltri,[23,aa] A. Venkateswaran,[45] M. Vesterinen,[52] D. Vieira,[61] M. Vieites Diaz,[44] X. Vilasis-Cardona,[40] E. Vilella Figueras,[56] A. Villa,[21] P. Vincent,[14] F. C. Volle,[12] D. vom Bruch,[11] V. Vorobyev,[39] N. Voropaev,[39] K. Vos,[76] C. Vrahas,[54] J. Walsh,[30] E. J. Walton,[65,52] G. Wan,[5] C. Wang,[18] G. Wang,[7] J. Wang,[5] J. Wang,[4] J. Wang,[3] J. Wang,[70] M. Wang,[26] N. W. Wang,[6] R. Wang,[50] X. Wang,[68] Y. Wang,[7] Z. Wang,[46] Z. Wang,[3] Z. Wang,[6] J. A. Ward,[52,65] N. K. Watson,[49] D. Websdale,[57] Y. Wei,[5] B. D. C. Westhenry,[50] D. J. White,[58] M. Whitehead,[55] A. R. Wiederhold,[52] D. Wiedner,[16] G. Wilkinson,[59] M. K. Wilkinson,[61] I. Williams,[51] M. Williams,[60] M. R. J. Williams,[54] R. Williams,[51] F. F. Wilson,[53] W. Wislicki,[37] M. Witek,[36] L. Witola,[18] C. P. Wong,[63] G. Wormser,[12] S. A. Wotton,[51] H. Wu,[64] J. Wu,[7] Y. Wu,[5] K. Wyllie,[44] S. Xian,[68] Z. Xiang,[4] Y. Xie,[7] A. Xu,[30] J. Xu,[6] L. Xu,[3] L. Xu,[3] M. Xu,[52] Z. Xu,[10] Z. Xu,[6] Z. Xu,[4] D. Yang,[3] S. Yang,[6] X. Yang,[5] Y. Yang,[25,i] Z. Yang,[5] Z. Yang,[62] V. Yeroshenko,[12] H. Yeung,[58] H. Yin,[7] C. Y. Yu,[5] J. Yu,[67] X. Yuan,[4] E. Zaffaroni,[45] M. Zavertyaev,[17] M. Zdybal,[36] M. Zeng,[3] C. Zhang,[5] D. Zhang,[7] J. Zhang,[6] L. Zhang,[3] S. Zhang,[67] S. Zhang,[5] Y. Zhang,[5] Y. Zhang,[59] Y. Z. Zhang,[3] Y. Zhao,[18] A. Zharkova,[39] A. Zhelezov,[18] X. Z. Zheng,[3] Y. Zheng,[6] T. Zhou,[5] X. Zhou,[7] Y. Zhou,[6] V. Zhovkovska,[12] L. Z. Zhu,[6] X. Zhu,[3] X. Zhu,[7] Z. Zhu,[6] V. Zhukov,[15,39] J. Zhuo,[43] Q. Zou,[4,6] S. Zucchelli,[21,h] D. Zuliani,[29,f] and G. Zunica[58]

(LHCb Collaboration)

[1]Centro Brasileiro de Pesquisas Físicas (CBPF), Rio de Janeiro, Brazil
[2]Universidade Federal do Rio de Janeiro (UFRJ), Rio de Janeiro, Brazil
[3]Center for High Energy Physics, Tsinghua University, Beijing, China
[4]Institute Of High Energy Physics (IHEP), Beijing, China
[5]School of Physics State Key Laboratory of Nuclear Physics and Technology, Peking University, Beijing, China
[6]University of Chinese Academy of Sciences, Beijing, China
[7]Institute of Particle Physics, Central China Normal University, Wuhan, Hubei, China
[8]Consejo Nacional de Rectores (CONARE), San Jose, Costa Rica
[9]Université Savoie Mont Blanc, CNRS, IN2P3-LAPP, Annecy, France
[10]Université Clermont Auvergne, CNRS/IN2P3, LPC, Clermont-Ferrand, France
[11]Aix Marseille Univ, CNRS/IN2P3, CPPM, Marseille, France
[12]Université Paris-Saclay, CNRS/IN2P3, IJCLab, Orsay, France
[13]Laboratoire Leprince-Ringuet, CNRS/IN2P3, Ecole Polytechnique, Institut Polytechnique de Paris, Palaiseau, France
[14]LPNHE, Sorbonne Université, Paris Diderot Sorbonne Paris Cité, CNRS/IN2P3, Paris, France
[15]I. Physikalisches Institut, RWTH Aachen University, Aachen, Germany
[16]Fakultät Physik, Technische Universität Dortmund, Dortmund, Germany
[17]Max-Planck-Institut für Kernphysik (MPIK), Heidelberg, Germany
[18]Physikalisches Institut, Ruprecht-Karls-Universität Heidelberg, Heidelberg, Germany
[19]School of Physics, University College Dublin, Dublin, Ireland
[20]INFN Sezione di Bari, Bari, Italy

[21]INFN Sezione di Bologna, Bologna, Italy
[22]INFN Sezione di Ferrara, Ferrara, Italy
[23]INFN Sezione di Firenze, Firenze, Italy
[24]INFN Laboratori Nazionali di Frascati, Frascati, Italy
[25]INFN Sezione di Genova, Genova, Italy
[26]INFN Sezione di Milano, Milano, Italy
[27]INFN Sezione di Milano-Bicocca, Milano, Italy
[28]INFN Sezione di Cagliari, Monserrato, Italy
[29]INFN Sezione di Padova, Padova, Italy
[30]INFN Sezione di Pisa, Pisa, Italy
[31]INFN Sezione di Roma La Sapienza, Roma, Italy
[32]INFN Sezione di Roma Tor Vergata, Roma, Italy
[33]Nikhef National Institute for Subatomic Physics, Amsterdam, Netherlands
[34]Nikhef National Institute for Subatomic Physics and VU University Amsterdam, Amsterdam, Netherlands
[35]AGH - University of Krakow, Faculty of Physics and Applied Computer Science, Kraków, Poland
[36]Henryk Niewodniczanski Institute of Nuclear Physics Polish Academy of Sciences, Kraków, Poland
[37]National Center for Nuclear Research (NCBJ), Warsaw, Poland
[38]Horia Hulubei National Institute of Physics and Nuclear Engineering, Bucharest-Magurele, Romania
[39]Affiliated with an institute covered by a cooperation agreement with CERN
[40]DS4DS, La Salle, Universitat Ramon Llull, Barcelona, Spain
[41]ICCUB, Universitat de Barcelona, Barcelona, Spain
[42]Instituto Galego de Física de Altas Enerxías (IGFAE), Universidade de Santiago de Compostela, Santiago de Compostela, Spain
[43]Instituto de Fisica Corpuscular, Centro Mixto Universidad de Valencia - CSIC, Valencia, Spain
[44]European Organization for Nuclear Research (CERN), Geneva, Switzerland
[45]Institute of Physics, Ecole Polytechnique Fédérale de Lausanne (EPFL), Lausanne, Switzerland
[46]Physik-Institut, Universität Zürich, Zürich, Switzerland
[47]NSC Kharkiv Institute of Physics and Technology (NSC KIPT), Kharkiv, Ukraine
[48]Institute for Nuclear Research of the National Academy of Sciences (KINR), Kyiv, Ukraine
[49]University of Birmingham, Birmingham, United Kingdom
[50]H.H. Wills Physics Laboratory, University of Bristol, Bristol, United Kingdom
[51]Cavendish Laboratory, University of Cambridge, Cambridge, United Kingdom
[52]Department of Physics, University of Warwick, Coventry, United Kingdom
[53]STFC Rutherford Appleton Laboratory, Didcot, United Kingdom
[54]School of Physics and Astronomy, University of Edinburgh, Edinburgh, United Kingdom
[55]School of Physics and Astronomy, University of Glasgow, Glasgow, United Kingdom
[56]Oliver Lodge Laboratory, University of Liverpool, Liverpool, United Kingdom
[57]Imperial College London, London, United Kingdom
[58]Department of Physics and Astronomy, University of Manchester, Manchester, United Kingdom
[59]Department of Physics, University of Oxford, Oxford, United Kingdom
[60]Massachusetts Institute of Technology, Cambridge, MA, United States
[61]University of Cincinnati, Cincinnati, OH, United States
[62]University of Maryland, College Park, MD, United States
[63]Los Alamos National Laboratory (LANL), Los Alamos, NM, United States
[64]Syracuse University, Syracuse, NY, United States
[65]School of Physics and Astronomy, Monash University, Melbourne, Australia (associated with Department of Physics, University of Warwick, Coventry, United Kingdom)
[66]Pontifícia Universidade Católica do Rio de Janeiro (PUC-Rio), Rio de Janeiro, Brazil (associated with Universidade Federal do Rio de Janeiro (UFRJ), Rio de Janeiro, Brazil)
[67]School of Physics and Electronics, Hunan University, Changsha City, China (associated with Institute of Particle Physics, Central China Normal University, Wuhan, Hubei, China)
[68]Guangdong Provincial Key Laboratory of Nuclear Science, Guangdong-Hong Kong Joint Laboratory of Quantum Matter, Institute of Quantum Matter, South China Normal University, Guangzhou, China (associated with Center for High Energy Physics, Tsinghua University, Beijing, China)
[69]Lanzhou University, Lanzhou, China (associated with Institute Of High Energy Physics (IHEP), Beijing, China)
[70]School of Physics and Technology, Wuhan University, Wuhan, China (associated with Center for High Energy Physics, Tsinghua University, Beijing, China)

[71]*Departamento de Fisica, Universidad Nacional de Colombia, Bogota, Colombia (associated with LPNHE, Sorbonne Université, Paris Diderot Sorbonne Paris Cité, CNRS/IN2P3, Paris, France)*
[72]*Universität Bonn - Helmholtz-Institut für Strahlen und Kernphysik, Bonn, Germany (associated with Physikalisches Institut, Ruprecht-Karls-Universität Heidelberg, Heidelberg, Germany)*
[73]*Eotvos Lorand University, Budapest, Hungary (associated with European Organization for Nuclear Research (CERN), Geneva, Switzerland)*
[74]*INFN Sezione di Perugia, Perugia, Italy (associated with INFN Sezione di Ferrara, Ferrara, Italy)*
[75]*Van Swinderen Institute, University of Groningen, Groningen, Netherlands (associated with Nikhef National Institute for Subatomic Physics, Amsterdam, Netherlands)*
[76]*Universiteit Maastricht, Maastricht, Netherlands (associated with Nikhef National Institute for Subatomic Physics, Amsterdam, Netherlands)*
[77]*Tadeusz Kosciuszko Cracow University of Technology, Cracow, Poland (associated with Henryk Niewodniczanski Institute of Nuclear Physics Polish Academy of Sciences, Kraków, Poland)*
[78]*Department of Physics and Astronomy, Uppsala University, Uppsala, Sweden (associated with School of Physics and Astronomy, University of Glasgow, Glasgow, United Kingdom)*
[79]*University of Michigan, Ann Arbor, MI, United States (associated with Syracuse University, Syracuse, NY, United States)*
[80]*Departement de Physique Nucleaire (SPhN), Gif-Sur-Yvette, France*

[a]Deceased.
[b]Also at Università di Roma Tor Vergata, Roma, Italy.
[c]Also at Università di Firenze, Firenze, Italy.
[d]Also at Scuola Normale Superiore, Pisa, Italy.
[e]Also at Università di Ferrara, Ferrara, Italy.
[f]Also at Università di Padova, Padova, Italy.
[g]Also at Università di Milano Bicocca, Milano, Italy.
[h]Also at Università di Bologna, Bologna, Italy.
[i]Also at Università di Genova, Genova, Italy.
[j]Also at Università degli Studi di Milano, Milano, Italy.
[k]Also at Universidade da Coruña, Coruña, Spain.
[l]Also at Universidad Nacional Autónoma de Honduras, Tegucigalpa, Honduras.
[m]Also at Università di Cagliari, Cagliari, Italy.
[n]Also at Centro Federal de Educacão Tecnológica Celso Suckow da Fonseca, Rio De Janeiro, Brazil.
[o]Also at Università di Bari, Bari, Italy.
[p]Also at Università di Perugia, Perugia, Italy.
[q]Also at LIP6, Sorbonne Universite, Paris, France.
[r]Also at Universidade Federal do Triângulo Mineiro (UFTM), Uberaba-MG, Brazil.
[s]Also at Universidade de Brasília, Brasília, Brazil.
[t]Also at Hangzhou Institute for Advanced Study, UCAS, Hangzhou, China.
[u]Also at Università di Pisa, Pisa, Italy.
[v]Also at Central South U., Changsha, China.
[w]Also at Excellence Cluster ORIGINS, Munich, Germany.
[x]Also at Università della Basilicata, Potenza, Italy.
[y]Also at Università di Siena, Siena, Italy.
[z]Also at Universidad de Alcalá, Alcalá de Henares, Spain.
[aa]Also at Università di Urbino, Urbino, Italy.